AD_____

Award Number: W81XWH-04-1-0704

TITLE: Development of a Novel Prognostic Marker to Link a Potential Tumor Suppressor Gene at Chromosome 6q to Aberrant Signal Transduction Pathway in Breast Cancer

PRINCIPAL INVESTIGATOR: Pan Zheng, M.D., Ph.D.

CONTRACTING ORGANIZATION: Ohio State University Research Foundation
Columbus, OH 43210-1063

REPORT DATE: August 2005

TYPE OF REPORT: Final

20060223 001

PREPARED FOR: U.S. Army Medical Research and Materiel Command
Fort Detrick, Maryland 21702-5012

DISTRIBUTION STATEMENT: Approved for Public Release;
Distribution Unlimited

The views, opinions and/or findings contained in this report are those of the author(s) and should not be construed as an official Department of the Army position, policy or decision unless so designated by other documentation.

REPORT DOCUMENTATION PAGE		Form Approved OMB No. 0704-0188

Public reporting burden for this collection of information is estimated to average 1 hour per response, including the time for reviewing instructions, searching existing data sources, gathering and maintaining the data needed, and completing and reviewing this collection of information. Send comments regarding this burden estimate or any other aspect of this collection of information, including suggestions for reducing this burden to Department of Defense, Washington Headquarters Services, Directorate for Information Operations and Reports (0704-0188), 1215 Jefferson Davis Highway, Suite 1204, Arlington, VA 22202-4302. Respondents should be aware that notwithstanding any other provision of law, no person shall be subject to any penalty for failing to comply with a collection of information if it does not display a currently valid OMB control number. **PLEASE DO NOT RETURN YOUR FORM TO THE ABOVE ADDRESS.**

1. REPORT DATE (DD-MM-YYYY) 01-08-05	2. REPORT TYPE Final	3. DATES COVERED (From - To) 07/15/04-07/14/05

4. TITLE AND SUBTITLE	5a. CONTRACT NUMBER
Development of a Novel Prognostic Marker to Link a Potential Tumor Suppressor Gene at Chromosome 6q to Aberrant Signal Transduction Pathway in Breast Cancer	5b. GRANT NUMBER W81XWH-04-1-0704
	5c. PROGRAM ELEMENT NUMBER

6. AUTHOR(S)	5d. PROJECT NUMBER
Pan Zheng, M.D., Ph.D.	5e. TASK NUMBER
	5f. WORK UNIT NUMBER
Email – zheng-1@medctr.osu.edu	

7. PERFORMING ORGANIZATION NAME(S) AND ADDRESS(ES)	8. PERFORMING ORGANIZATION REPORT NUMBER
Ohio State University Research Foundation Columbus, OH 43210-1063	

9. SPONSORING / MONITORING AGENCY NAME(S) AND ADDRESS(ES)	10. SPONSOR/MONITOR'S ACRONYM(S)
U.S. Army Medical Research and Materiel Command Fort Detrick, Maryland 21702-5012	
	11. SPONSOR/MONITOR'S REPORT NUMBER(S)

12. DISTRIBUTION / AVAILABILITY STATEMENT
Approved for Public Release; Distribution Unlimited

13. SUPPLEMENTARY NOTES

14. ABSTRACT:

Abstract can be found on next page.

15. SUBJECT TERMS
cancer suppressor gene, protein phosphatase, Wnt signaling pathway, loss of heterozygosity

16. SECURITY CLASSIFICATION OF:			17. LIMITATION OF ABSTRACT	18. NUMBER OF PAGES	19a. NAME OF RESPONSIBLE PERSON USAMRMC
a. REPORT U	b. ABSTRACT U	c. THIS PAGE U	UU	85	19b. TELEPHONE NUMBER (include area code) 301-619-7325

Standard Form 298 (Rev. 8-98)
Prescribed by ANSI Std. Z39.18

ABSTRACT

This is the final report on the grant "Development of a novel diagnostic marker to link a potential tumor suppressor gene at chromosome 6q to aberrant signal transduction pathway in breast cancer". The purpose of the grant proposal is to examine the hypothesis that protein phosphatase laforin is a tumor suppressor in cancers through its function as the specific phosphatase of GSK-3β and the loss of function of laforin causes aberrant Wnt signaling in cancer cells. We have proposed to examine (1) whether the specific marker is present in breast cancer cells; (2) whether the unique morphological marker correlates with specific LOH in 6q24; (3) whether there are inactivating mutations in laforin gene; (4) whether loss of laforin function in breast cancer cells causes downstream effects on β-catenin cytosolic and nuclear accumulation and increased cyclin D and c-myc expression in breast cancer samples. (5) Finally, we will examine whether loss of laforin function in breast cancer cells is an independent prognostic factor. In the past funding period, we have greatly extended our work in basic research to firmly establish the role of laforin as a tumor suppressor. First, we showed that silencing the *Epm2a* gene (which encodes laforin) in the bone marrow stem cells resulted in a dramatic increase in the self-renewal of the hematopoietic stem cells in methylcellulose assay in vitro and in the tendency for hematological malignancy transformation in vivo. Second, we have demonstrated that abnormal Wnt signaling associated with laforin down-regulation is a causal event for the malignant transformation mediated by laforin-down regulation.

Table of Contents

(4) Introduction

Glycogen synthase kinase 3 (GSK-3) is a critical component for several important signal transduction pathways that control cellular metabolism, growth, and transformation. GSK-3 targets a wide array of substrates that are implicated in human cancer and other diseases. GSK-3β kinase is inactivated by phosphorylation, specifically at serine 9 by protein kinase B/Akt. A counteracting phosphatase for this has not been identified. Our study showed that laforin, a dual-specificity phosphatase which is mutated in Lafora's progressive myoclonus epilepsy, is the phosphatase for GSK-3β and an important modulator in Wnt signalling pathway. Moreover, laforin is a tumor suppressor as disruption of its expression leads to development of tumor, while its over-expression suppresses tumor growth.

Laforin is a potential tumor suppressor.

Tumor suppressor genes (TSG) form a crucial part of our natural anticancer defense. When these genes become inactive, tumors often develop. Knudson's two-hit model of tumor suppressor genes supposed that loss of function only occurs when both alleles of the gene are inactivated genetically (1, 2). Despite changes in our concept of cancer genes, two inactivating point mutations are still considered the hallmark of TSG (3). Recently more and more reports describe candidate TSGs that do not conform to this standard definition, including haploinsufficient genes requiring inactivation of only one allele and genes inactivated not by mutation but rather epigenetic hypermethylation (4-7).

Our preliminary studies strongly suggest that *EPM2A* is a potential tumor suppressor gene in the mouse. First, disruption of *EPM2A* gene leads to the development of lymphoma in essentially 100% of B10BR mice. Second, our analysis of the status of the *EPM2A* gene revealed wide-spread hypermethylation in its 5'CpG island. Third, transfection of *EPM2A* cDNA into a large panel of tumor cells lead to programmed cell death. However, there is a significant difference in tumor incidence when the transgene is presented in the B10.BR x B6 background. These results suggest that the cancer risk associated with the *EPM2A* disruption can be modified by other background genes yet to be identified. The strong effect of background genes may explain the apparent lack of tumors in the B6 mice with targeted mutation of the *EPM2A* gene (8).

High frequency of LOH is found in 6q24 region in breast cancers

Laforin gene EPM2A is located in 6q24 in human genome (9-11). The long arm of chromosome 6 is frequently rearranged in human cancer. Deletions or LOH in 6q were reported in cancers from a large number of different organs including carcinomas of the breast (12, 13), endometrium (14, 15), prostate (16), lymphomas and leukemias (17), and melanomas (18). The frequent genetic changes in various cancers strongly suggests the existence of putative tumor suppressor genes (TSGs) in chromosome 6q.

Deletions on chromosome 6q21-qter and 1p22-36 were two most frequent karyotypic abnormalities in a survey of 508 breast carcinomas (19). Frequent loss at 6q was confirmed by comparative genomic hybridization (20) and allelotying of human breast carcinomas (21). Studies using a large number of microsatellite markers suggested the presence of at least three regions of frequent allelic imbalance at 6q13, 6q24-q25, and 6q27 (12, 21-23). A study with microdissected breast cancer tissues indicated that allelic loss at 6q23-q25.2 could be observed in up to 80% of the samples (24). Microcell-mediated chromosomal transfer experiments using a 6q portion demarcated by the microsatellite marker D6S310 (6q23.3-q25) caused suppression of the neoplastic

4

phenotype in vitro and in vivo of CAL51 breast cancer cells (23). All these data indicated that chromosomal 6q is likely to harbor several TSGs and that 6q23-q25 is an important hot spot in breast cancer.

(5) Body of Annual Report

Task 1. Are there Lafora bodies in breast cancer cells? (Month 1-12).
a. To obtain more tissue microarray sections to perform the following histological staining procedures: PAS, PAS-D, PAS/alcian blue, Hale's PAS, Best's carmine, dimedone-PAS, Congo red, Sudan IV. (Month 1-2).
b. To retrieve the tissue blocks and make thick sections for Laser Captured Microdissection from the paired tumor and normal tissue (Month 1-4).
c. To submit mouse lymphoma samples to perform electronic microscopy examination (Month 1-3)
d. To procure properly fixed breast cancer tissue to perform electronic microscopy examination (Month 1-12).
e. To retrieve tissue blocks with benign breast lesions and perform various histological staining procedures (Month 1-6).

We have finished the task 1 with more detailed histological examinations on PAS-D positive intracellular inclusions that we identified in breast cancer samples of which we speculated in grant proposal as "lafora's bodies" (Fig. 1 and Fig. 2). We performed electron microscopy examination on mouse lymphoma tissue sections from TG-B mice and on human breast cancer samples (Fig. 3).
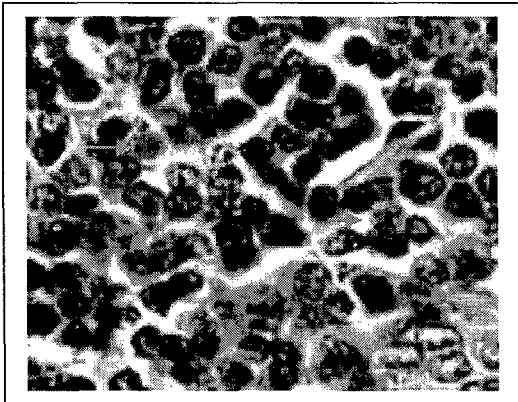

Fig. 1. Intracellular PAS-D positive inclusions were seen in lymphoma cells from a lymph node of a TG-B mouse that developed lymphoma. Paraffin-embedded tissue was stained with PAS with diastase digestion. Arrows showed two round purple intracellular PAS-D positive inclusions.

Fig. 2. Intracellular PAS-D positive inclusions in ductal carcinoma of the breast. (100X objective). Arrows indicated the larger inclusions. Numerous smaller inclusions are also present.
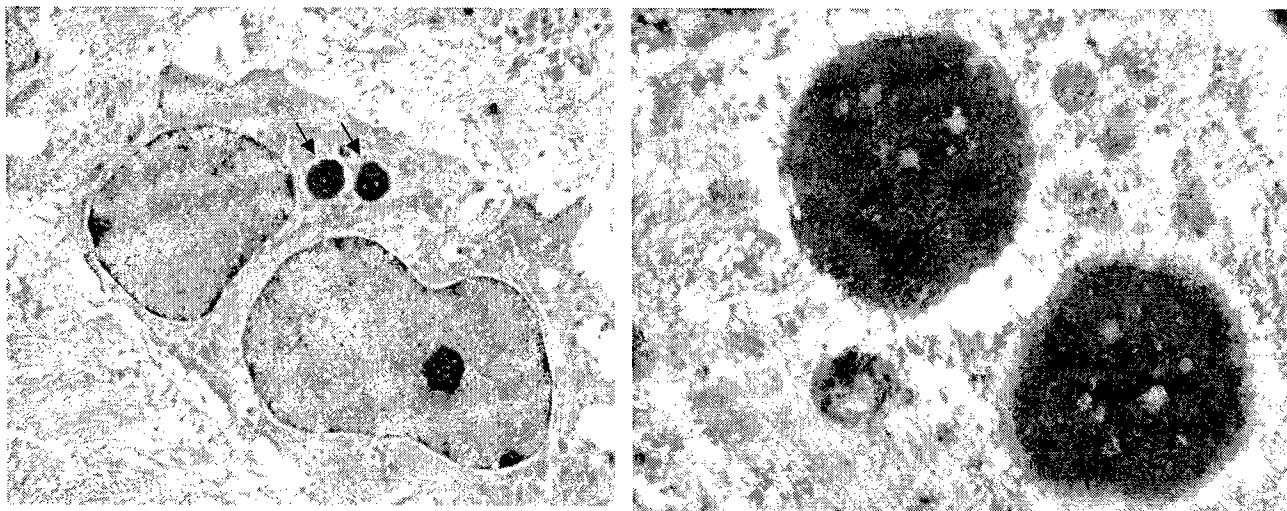
5

Fig. 3. Preliminary result of electron microscopy pictures of PAS-D positive intracytoplasmic inclusion bodies in breast cancer cells. These inclusions are electronic dense granules and no limiting membrane. However, there is no apparent filamentous material. The right panel is a higher power view of the structures indicated by arrows on the left panel.

From the careful analysis of histochemical studies and electron microscopy results, we came to the conclusion that the PAS-D positive intracellular inclusions in lymphoma and breast cancer cells that we identified are different than the lafora bodies described in literature. The most reliable method to confirm whether the PAS-D positive inclusion is a Lafora body is electron microscopy (25). Ultrastructurally, Lafora bodies are said to be composed of amorphous electron-dense granules and irregular filamentous material. They are not separated from other cytoplasmic components by a membrane. They are mostly located in juxtanuclear position, indented the nucleus. The inclusions are not related to the nuclear membrane or to the endoplasmic reticulum. We failed to identify any filamentous material.

Task 2. Is the marker correlated with genomic instability? (Month 3-12).
a. To obtain benign tissue by simple scraping (Month 3-4).
b. To obtain tumor tissue by laser captured microdissection on all 50 tumor samples to ensure the purity of tumor cells (Month 3-8).
c. To isolate DNA and amplify DNA for alleletyping (Month 3-8).
d. To perform PCR amplification with microsatellite markers and send to Genotyping Core Facility for alleletyping (Month 4-12).
e. To collect and analyze data, perform statistical study (Month 9-12).

We have chosen 2 microsatellite markers to evaluate the LOH at 6q24 region. The markers are list in Table 1. D6S1703 is the marker that has been used for the positional cloning of laforin gene EPM2A. It's located in the first intron of the EPM2A gene. Rodriguez et al have analyzed 30 microsatellite markers mapping in the 6q13-27 region

6

on a panel of 178 breast cancer samples (26). Our two markers are also used by their report with allelic imbalance frequency: D6S1703, 28.7%; D6S441, 32.9%.

Table 1. Microsatellite markers in 6q24.

Marker Name	Sequence Position (Mbp)	Marshfield Position (cM)	PCR Product Size (bp)
D6S1703	145.95	146.06	147-161
D6S441	153.77	154.10	162-186

We have performed studies in 50 cases of ductal carcinoma of the breast. Cancer cells were microdissected after H&E staining. Paired normal tissue sections were scraped by clean blade and collected in PCR tube. DNA was isolated and amplified by whole genome amplification (27, 28). PCR reactions were performed and genotyped by Genotyping Service in our Comprehensive Cancer Center core facility. The allelic imbalance (AI) is determined by comparing the ratio of allele peak heights in tumor and control DNA (N1/N2)/(T1/T2), the LOH is defined as normal/tumor ratios, <0.7 or >1.5. Of the 34 informative samples using D6S1703, the marker that resides in the first intron of EPM2A gene, we found LOH in 21 samples, which accounts for 62% of the samples (Fig. 4). Since the marker D6S1703 is within the EPM2A gene, the preliminary data strongly suggest a wide-spread LOH in the EPM2A gene. We are currently adjusting the PCR amplification conditions and targeting to amplify all DNA samples with readable signals.
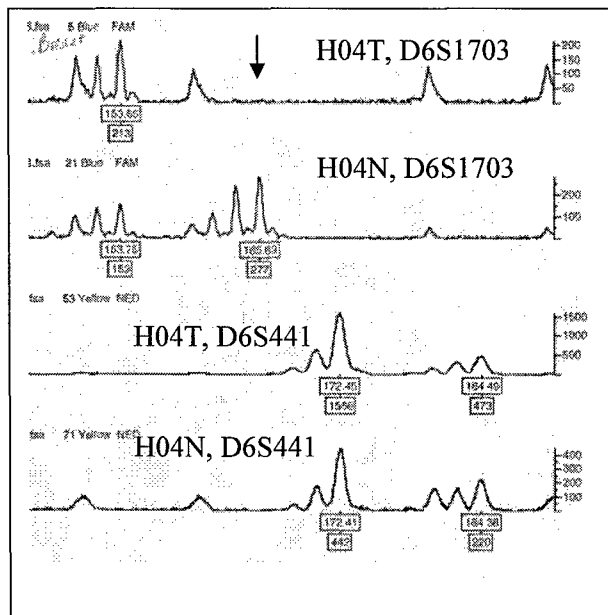

Fig. 4. LOH analysis of ductal carcinomas in breast using D6S1703 and D6S441 markers. N. Normal tissue, T, microdissected tumor cells. Arrow indicated the tumor cells had a complete loss of one allele at locus D6S1703.

The LOH results had been compared with PAS-D staining results. However, the LOH results were not matched with the PAS-D staining results. First, this may confirm our suspicion that what we observed as "intracellular PAS-D positive inclusions" were not exactly "Lafora bodies" even though we only observed such inclusions in ductal carcinoma cells but not on normal lobular glands or normal ducts. Second, it should be emphasized that Lafora bodies represent the loss of laforin function. This can be achieved

7

by either deletion of both copies of laforin gene, or LOH at one copy and inactivation mutation in another copy, or inactivation mutation in both copies. It can also be caused by epigenetic inhibition, transcription inhibition or other mechanisms. Thus, the LOH data may not exactly match the PAS-D inclusions samples. If we could successfully reveal two alleles in locus D6S1703 in normal tissue, but failed to amplify any allele from tumor cells while other markers are not affected, we may conclude that it is a deletion of both alleles in tumor cells. On the other hand, LOH at locus D6S1703 will prompt us to perform further careful searching on inactivating mutations in laforin gene from the remaining allele. In the case of homozygosity at locus D6S1703 with PAS-D inclusions, it may also make searching for inactivating mutations in laforin gene more significant.

Task 3. Can we identify inactivating mutations in laforin gene in breast cancer cells? (Month 7-12).
a. To isolate high quality DNA from paired tumor and normal tissue samples that is positive for PAS-D inclusions (Month 7-8).
b. To amplify the exons in laforin gene (Month 7-9).
c. To detect the presence of mutations by sequencing (Month 8-10).
d. To analyze the mutations (Month 11-12).

We are still in the process of doing Task 3. We encountered difficulty in getting good quality of genomic DNA from formalin fixed paraffin embedded tissue. The exon 1 of EPM2a gene is high GC rich and extremely difficult to amplify. Our preliminary data from 20 cases of ductal carcinoma of the breast indicated that there was no mutation identified so far.

Task 4. Are there hypermethylation in CpG island of laforin gene promoter and exon 1 region? (Month 7-12).
*   a. To design the oligonucleotide primers for methylation specific PCR and to optimize PCR conditions to specifically amplify the desired methylated or unmethylated PCR products (month 7-8).*
*   b. To isolate high quality DNA (month 7-8).*
*   c. To modify DNA with bisulfate treatment and perform methylation specific PCR (month 9-10).*
*   d. To analyze the results (Month 11-12).*

We are still in the process of doing Task 4. As described in Task 3, we encountered difficulty in getting good quality of genomic DNA from formalin fixed paraffin embedded tissue. That made the bisulfate treatment and methylation specific PCR almost impossible to get satisfactory results. We are currently trying hard to trouble shooting.

Task 5. What are the downstream effects on loss of laforin function? (Month 1-12)
a. To perform immunohistochemical staining to examine the GSK-3β; phosphorylation level, the increased β-catenin cytosolic and nuclear accumulation, increased cyclin D and c-myc expression in breast cancer samples (Month 1-12).

We have performed immunohistochemical stainnings with antibodies against β-catenin and c-myc on the breast cancer samples (Fig. 5). We are in the process of summarizing the results. We will compare the LOH results with the β-catenin and c-myc staining results to examine the correlations.
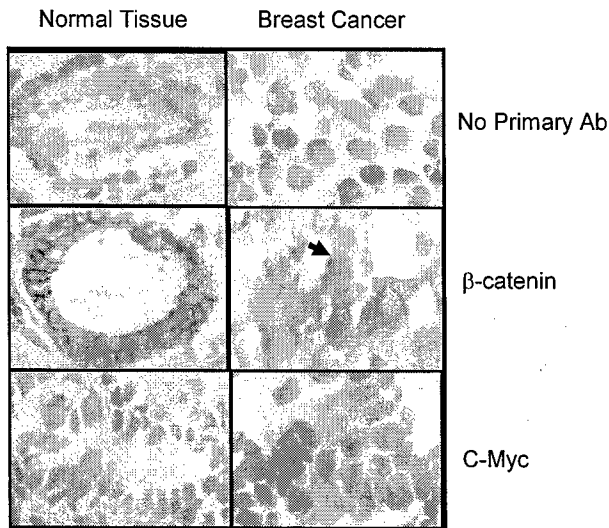
Normal Tissue	Breast Cancer	
		No Primary Ab
		β-catenin
		C-Myc

Fig. 5. Immunohistochemical studies in ductal carcinomas of the breast.

Task 6. Could positive for Lafora body be a prognostic factor? (Month 1-12)
a. To retrieve the consecutive series of breast cancer samples and pathological reports from 1981 to 1985 and perform the PAS-D stain on the sections to determine the frequency of PAS-D inclusion positive cases (Month 1-5).
b. To analyze the retrieved pathologic reports (Month 1-5)
c. If necessary, to perform immunohistochemical stains on ER, PR, p53, HER on all the cases that does not have such information (Month 4-7).
d. To obtain the survival data from the CDRS database (Month 4-12).
e. To correlate with pathological grading, clinical staging, and patients' survival data to determine whether loss of laforin function in breast cancer is an independent prognostic factor (Month 10-12).

We are in the process of doing this task, not complete.

9

(6) Key Research Accomplishments

- The major effort of the funding period is on the basic research to firmly establish the role of laforin as a tumor suppressor.
- We showed that silencing the *Epm2a* gene (which encodes laforin) in the bone marrow stem cells resulted in a dramatic increase in the self-renewal of the hematopoietic stem cells in methylcellulose assay in vitro and in the tendency for hematological malignancy transformation in vivo.
- We have demonstrated that abnormal Wnt signaling associated with laforin down-regulation is a causal event for the malignant transformation mediated by laforin-down regulation.
- We have performed loss of heterozygosity (LOH) analysis in 50 cases of ductal carcinoma of the breast. The results showed that LOH at the EPM2a gene locus was 62%.

(7) Reportable Outcomes:

1. Manuscript submitted to Cell (revision): Laforin is a phosphatase for glycogen synthase kinase-3β and suppresses tumor growth by modulating Wnt signaling. Attached as appendix.

2. Poster presentation by Pan Zheng at "Era of Hope 2005", June 8-11, 2005. Laforin is a phosphatase for glycogen synthase kinase-3β and suppresses tumor growth by modulating Wnt signaling.

(8) Conclusions:

In summary, we have made important progress during the one year funding period to achieve our goal. We have followed the Statement of Work closely. We have completed the Task 1, 2 and made important and promising progress in Task 3-6. Taken together, we made major effort on the basic research to firmly establish the role of laforin as a tumor suppressor. We showed that silencing the *Epm2a* gene (which encodes laforin) in the bone marrow stem cells resulted in a dramatic increase in the self-renewal of the hematopoietic stem cells in methylcellulose assay in vitro and in the tendency for hematological malignancy transformation in vivo. We have demonstrated that abnormal Wnt signaling associated with laforin down-regulation is a causal event for the malignant transformation mediated by laforin-down regulation. The results, together with our preliminary work in establishing laforin as the specific phosphatase for GSK-3b, have summarized in a manuscript that Cell reviewed and requested a revision. The revised manuscript is attached as appendix.

(9) References:

1.	Knudson, A. G., Jr. Mutation and cancer: statistical study of retinoblastoma. Proc Natl Acad Sci U S A 68:820-3. 1971.

2.	Knudson, A. G., Jr., Hethcote, H. W., and Brown, B. W. Mutation and childhood cancer: a probabilistic model for the incidence of retinoblastoma. Proc Natl Acad Sci U S A 72:5116-20. 1975.

3.	Hanahan, D., and Weinberg, R. A. The hallmarks of cancer. Cell 100:57-70. 2000.

4.	Haber, D., and Harlow, E. Tumour-suppressor genes: evolving definitions in the genomic age. Nat Genet 16:320-2. 1997.

5.	Paige, A. J. Redefining tumour suppressor genes: exceptions to the two-hit hypothesis. Cell Mol Life Sci 60:2147-63. 2003.

6.	Li, Q. L., Ito, K., Sakakura, C., Fukamachi, H., Inoue, K., Chi, X. Z., Lee, K. Y., Nomura, S., Lee, C. W., Han, S. B., Kim, H. M., Kim, W. J., Yamamoto, H., Yamashita, N., Yano, T., Ikeda, T., Itohara, S., Inazawa, J., Abe, T., Hagiwara, A., Yamagishi, H., Ooe, A., Kaneda, A., Sugimura, T., Ushijima, T., Bae, S. C., and Ito, Y. Causal relationship between the loss of RUNX3 expression and gastric cancer. Cell 109:113-24. 2002.

7.	Balmain, A. Cancer: new-age tumour suppressors. Nature 417:235-7. 2002.

8.	Ganesh, S., Delgado-Escueta, A. V., Sakamoto, T., Avila, M. R., Machado-Salas, J., Hoshii, Y., Akagi, T., Gomi, H., Suzuki, T., Amano, K., Agarwala, K. L., Hasegawa, Y., Bai, D. S., Ishihara, T., Hashikawa, T., Itohara, S., Cornford, E. M., Niki, H., and Yamakawa, K. Targeted disruption of the Epm2a gene causes formation of Lafora inclusion bodies, neurodegeneration, ataxia, myoclonus epilepsy and impaired behavioral response in mice. Hum Mol Genet 11:1251-62. 2002.

9.	Serratosa, J. M., Delgado-Escueta, A. V., Posada, I., Shih, S., Drury, I., Berciano, J., Zabala, J. A., Antunez, M. C., and Sparkes, R. S. The gene for progressive myoclonus epilepsy of the Lafora type maps to chromosome 6q. Hum Mol Genet 4:1657-63. 1995.

10.	Serratosa, J. M., Gomez-Garre, P., Gallardo, M. E., Anta, B., de Bernabe, D. B., Lindhout, D., Augustijn, P. B., Tassinari, C. A., Malafosse, R. M., Topcu, M., Grid, D., Dravet, C., Berkovic, S. F., and de Cordoba, S. R. A novel protein tyrosine phosphatase gene is mutated in progressive myoclonus epilepsy of the Lafora type (EPM2). Hum Mol Genet 8:345-52. 1999.

11.	Minassian, B. A., Lee, J. R., Herbrick, J. A., Huizenga, J., Soder, S., Mungall, A. J., Dunham, I., Gardner, R., Fong, C. Y., Carpenter, S., Jardim, L., Satishchandra, P., Andermann, E., Snead, O. C., 3rd, Lopes-Cendes, I., Tsui, L. C., Delgado-Escueta, A. V., Rouleau, G. A., and Scherer, S. W. Mutations in a gene encoding a novel protein tyrosine phosphatase cause progressive myoclonus epilepsy. Nat Genet 20:171-4. 1998.

12.	Sheng, Z. M., Marchetti, A., Buttitta, F., Champeme, M. H., Campani, D., Bistocchi, M., Lidereau, R., and Callahan, R. Multiple regions of chromosome 6q affected by loss of heterozygosity in primary human breast carcinomas. Br J Cancer 73:144-7. 1996.

13. Devilee, P., van Vliet, M., van Sloun, P., Kuipers Dijkshoorn, N., Hermans, J., Pearson, P. L., and Cornelisse, C. J. Allelotype of human breast carcinoma: a second major site for loss of heterozygosity is on chromosome 6q. Oncogene *6:*1705-11. 1991.

14. Tibiletti, M. G., Furlan, D., Taborelli, M., Facco, C., Riva, C., Franchi, M., Cossu, A., Trubia, M., Taramelli, R., and Capella, C. Microsatellite instability in endometrial cancer: relation to histological subtypes. Gynecol Oncol *73:*247-52. 1999.

15. Tibiletti, M. G., Bernasconi, B., Taborelli, M., Furlan, D., Fabbri, A., Franchi, M., Taramelli, R., Trubia, M., and Capella, C. Involvement of chromosome 6 in endometrial cancer. Br J Cancer *75:*1831-5. 1997.

16. Cooney, K. A., Wetzel, J. C., Consolino, C. M., and Wojno, K. J. Identification and characterization of proximal 6q deletions in prostate cancer. Cancer Res *56:*4150-3. 1996.

17. Gerard, B., Cave, H., Guidal, C., Dastugue, N., Vilmer, E., and Grandchamp, B. Delineation of a 6 cM commonly deleted region in childhood acute lymphoblastic leukemia on the 6q chromosomal arm. Leukemia *11:*228-32. 1997.

18. Walker, G. J., Palmer, J. M., Walters, M. K., Nancarrow, D. J., Parsons, P. G., and Hayward, N. K. Simple tandem repeat allelic deletions confirm the preferential loss of distal chromosome 6q in melanoma. Int J Cancer *58:*203-6. 1994.

19. Mertens, F., Johansson, B., Hoglund, M., and Mitelman, F. Chromosomal imbalance maps of malignant solid tumors: a cytogenetic survey of 3185 neoplasms. Cancer Res *57:*2765-80. 1997.

20. Nishizaki, T., DeVries, S., Chew, K., Goodson, W. H., 3rd, Ljung, B. M., Thor, A., and Waldman, F. M. Genetic alterations in primary breast cancers and their metastases: direct comparison using modified comparative genomic hybridization. Genes Chromosomes Cancer *19:*267-72. 1997.

21. Noviello, C., Courjal, F., and Theillet, C. Loss of heterozygosity on the long arm of chromosome 6 in breast cancer: possibly four regions of deletion. Clin Cancer Res *2:*1601-6. 1996.

22. Orphanos, V., McGown, G., Hey, Y., Boyle, J. M., and Santibanez-Koref, M. Proximal 6q, a region showing allele loss in primary breast cancer. Br J Cancer *71:*290-3. 1995.

23. Theile, M., Seitz, S., Arnold, W., Jandrig, B., Frege, R., Schlag, P. M., Haensch, W., Guski, H., Winzer, K. J., Barrett, J. C., and Scherneck, S. A defined chromosome 6q fragment (at D6S310) harbors a putative tumor suppressor gene for breast cancer. Oncogene *13:*677-85. 1996.

24. Fujii, H., Zhou, W., and Gabrielson, E. Detection of frequent allelic loss of 6q23-q25.2 in microdissected human breast cancer tissues. Genes Chromosomes Cancer *16:*35-9. 1996.

25. Van Hoof, F., and Hageman-Bal, M. Progressive familial myoclonic epilepsy with Lafora bodies. Electron microscopic and histochemical study of a cerebral biopsy. Acta Neuropathol (Berl) *7:*315-36. 1967.

26. Rodriguez, C., Causse, A., Ursule, E., and Theillet, C. At least five regions of imbalance on 6q in breast tumors, combining losses and gains. Genes Chromosomes Cancer *27:*76-84. 2000.

27. Dietmaier, W., Hartmann, A., Wallinger, S., Heinmoller, E., Kerner, T., Endl, E., Jauch, K. W., Hofstadter, F., and Ruschoff, J. Multiple mutation analyses in single tumor cells with improved whole genome amplification. Am J Pathol *154:*83-95. 1999.

28. Wang, V. W., Bell, D. A., Berkowitz, R. S., and Mok, S. C. Whole genome amplification and high-throughput allelotyping identified five distinct deletion regions on chromosomes 5 and 6 in microdissected early-stage ovarian tumors. Cancer Res *61:*4169-74. 2001.

Title: Laforin is a phosphatase for glycogen synthase kinase-3 beta and suppresses tumor growth by modulating Wnt signaling

Corresponding Author: Pan Zheng, MD, PhD

Corresponding Author's Institution: The Ohio State University

First Author: Ying Wang, PhD

Order of Authors: Ying Wang, PhD; Yan Liu, PhD; Cindy Wu; Huiming Zhang; Xincheng Zheng, MD; Zhi Zheng, PhD; Terrence L Geiger, MD, PhD; Yang Liu, PhD; Pan Zheng, MD, PhD

Manuscript Region of Origin:

Abstract: Glycogen synthase kinase 3 (GSK-3) is a critical component for several important signal transduction pathways that control cellular metabolism, growth, and transformation. GSK-3 targets a wide array of substrates that are implicated in human cancer and other diseases. GSK-3β kinase is inactivated by phosphorylation, specifically at serine 9 by protein kinase B/Akt. A counteracting phosphatase for this has not been identified. Here we report that laforin, a dual-specificity phosphatase which is mutated in Lafora's progressive myoclonus epilepsy, is a phosphatase for GSK-3β and an important modulator in Wnt signaling pathway. Moreover, laforin is a tumor suppressor as disruption of its expression leads to development of tumor, while its over-expression suppresses tumor growth.

Laforin is a phosphatase for glycogen synthase kinase-3β and suppresses tumor growth by modulating Wnt signaling

Yin Wang[1#], Yan Liu[1#], Cindy Wu,[1] Huiming Zhang[1], Xincheng Zheng[1], Zhi Zheng[2],

Terrence L. Geiger[3], Yang Liu[1*] and Pan Zheng[1*]

[1]Division of Cancer Immunology, Department of Pathology and Comprehensive Cancer

Center, Ohio State University Medical Center, Columbus, OH 43210

[3]Department of Pathology, St. Jude Children's Research Hospital, Memphis, TN 38105

[#]These authors contributed equally to this work.

[2]Current address: 289 Merrill Ave, Fremont, CA 94539.

*Correspondence and requests for materials should be addressed to:

Pan Zheng and Yang Liu

Division of Cancer Immunology, Department of Pathology, Ohio State University Medical

Center, 129 Hamilton Hall, 1645 Neil Avenue, Columbus, OH 43210.

PH: 614-292-2003; FAX: 614-688-8152; e-mail: zheng-1@medctr.osu.edu or liu-3@medctr.osu.edu

Summary

Glycogen synthase kinase 3 (GSK-3) is a critical component for several important signal transduction pathways that control cellular metabolism, growth, and transformation. GSK-3 targets a wide array of substrates that are implicated in human cancer and other diseases. GSK-3β kinase is inactivated by phosphorylation, specifically at serine 9 by protein kinase B/Akt. A counteracting phosphatase for this has not been identified. Here we report that laforin, a dual-specificity phosphatase which is mutated in Lafora's progressive myoclonus epilepsy, is a phosphatase for GSK-3β and an important modulator in Wnt signaling pathway. Moreover, laforin is a tumor suppressor as disruption of its expression leads to development of tumor, while its over-expression suppresses tumor growth.

2

Introduction

GSK-3 was discovered over 20 years ago as one of several protein kinases that phosphorylated and inactivated glycogen synthase (Cohen and Frame, 2001; Frame and Cohen, 2001). Accumulating evidence demonstrates that GSK-3 is involved in a wide range of cellular processes, ranging from glycogen metabolism to cell cycle regulation and proliferation (Doble and Woodgett, 2003; Manoukian and Woodgett, 2002; Woodgett, 2001). GSK-3β activity is regulated by phosphorylation. GSK-3β kinase is constitutively active in resting cells and is inactivated by phosphorylation at Ser 9 position by kinases such as protein kinase B (PKB)/Akt upon stimulation by insulin or growth factors (Alessi and Downes, 1998; Alessi et al., 1997b; Cross et al., 1995). Although a phosphatase specific for the Ser 9 position should positively regulate GSK-3β activity, no specific phosphatase has been identified.

GSK-3β is also a major component of the Wnt signaling pathway that influences cell growth, differentiation, migration and fate (Miller, 2002; Peifer and Polakis, 2000; Polakis, 2000). In this pathway, β-catenin mediates the transmission of a Wnt signal into the nucleus and the subsequent activation of target genes (Behrens et al., 1996; Bhanot et al., 1996; He et al., 1997; Molenaar et al., 1996). In the absence of Wnt signals, a cytoplasmic protein complex, consisting of Axin, APC, β-catenin, GSK-3β, protein phosphatase 2Ac, Dishevelled and casein kinase I, promotes the ubiquitination and subsequent degradation of β-catenin via the proteasome (Ikeda et al., 1998; Peifer and Polakis, 2000; Zeng et al., 1997). GSK-3β phosphorylates the critical residues in the N-terminal region of β-catenin that are essential for its binding to β-TrCP that leads to the protein degradation of β-catenin (Amit et al., 2002; Liu

et al., 2002; Yanagawa et al., 2002) . Mutations in β-catenin affecting the phosphorylation are found in a variety of human cancers (Polakis, 2000). Interestingly, Ding et al. suggested that phosphorylation of GSK-3β at Ser 9 is neither necessary nor sufficient for Wnt signaling (Ding et al., 2000). In support of this notion, mice with knock-in of the GSK3 mutants lacking the critical phosphorylation sites (Ser21 for α and Ser 9 for β) had a normal response to Wnt, but reduced glycogen synthase response to insulin (McManus et al., 2005). This suggestion, however, does not fully explain several lines of observations. First, a mutation in the GSK-3β Arg96 (R96A) that disrupts the binding pocket for the priming phosphate markedly increased β-catenin accumulation (Hagen et al., 2002). Second, several reports showed a critical role for the priming phosphorylation of β-catenin in Wnt signaling (Amit et al., 2002; Liu et al., 2002; Yanagawa et al., 2002). Since the Ser 9 blocks the GSK-3β pocket for the priming phosphate (Dajani et al., 2001; Frame et al., 2001), it is likely that the Ser 9 phosphorylation modulates Wnt signaling. In support of this notion, Ossipova et al. reported that LKB1/XEEK1, a tumor suppressor gene, regulates Wnt signaling by modulating GSK-3β phosphorylation at Ser 9 (Ossipova et al., 2003). It is therefore possible that Ser 9 or Ser 21 phosphorylation of GSK-3 may regulate Wnt signaling under some, although not all, circumstances. However, no phosphatase has been identified that directly regulates GSK-3β Ser 9 phosphorylation in the Wnt signaling pathway.

The *EPM2a* gene was first identified as its mutation causes Lafora's progressive myoclonus epilepsy, an uncommon neurological disorder usually fatal before the patient reaches 20 years of age (Minassian, 2001; Minassian, 2002; Minassian et al., 1998; Serratosa et al., 1999a; Serratosa et al., 1999b). Recent studies have demonstrated that *EPM2a* gene encodes a dual-specific phosphatase and that mutations in either the kinase domain or its

4

carbohydrate-binding domain can be found in patients (Wang et al., 2002). Although defects in the *EPM2a* gene have not been implicated in cancers, *EPM2a* is located in 6q24 of the human genome (Minassian et al., 1998; Serratosa et al., 1995; Serratosa et al., 1999b) where deletions or LOH were reported in cancers from a large number of different organs including carcinomas of the breast (Devilee et al., 1991; Sheng et al., 1996), endometrium (Tibiletti et al., 1997; Tibiletti et al., 1999), prostate (Cooney et al., 1996), lymphomas and leukemias including AIDS-associated lymphoma(Gerard et al., 1997; Pastore et al., 1996; Zhang et al., 1997), and melanomas(Walker et al., 1994).

The T cell receptor (TCR) transgenic mice have random co-integration of the genes encoding for the α and β chains of the TCR into the genome. Because of the allelic exclusion, expression of the transgenic TCR represses the endogenous TCR repertoire and renders mice deficient in T cell immunity to tumors and infections. The immunodeficiency may be responsible for the fact that some TCR transgenic mice have low incidence of thymoma late in life (around 2 years of age) (Reimann et al., 1994). We made a serendipitous observation that one line of B10.BR TCR transgenic mice, called TG-B mice(Geiger et al., 1992), developed T cell lymphoma with almost 100% penetrance within 6 months. By position cloning, we found that the transgenes were inserted in intron 1 of the *EPM2a* gene and caused its inactivation. These observations prompted us to study the function of laforin in signal transduction of tumorigenesis. Here we report that laforin is the phosphatase for GSK-3β, an important modulator of Wnt signaling and a tumor suppressor.

5

Results

Transgene insertion to and hypermethylation of *EPM2a* gene induces spontaneous lymphoma in TG-B transgenic mice

The TG-B transgenic mice used in this study have rearranged T cell receptor α and β-chain genes isolated from a clonal CD8$^+$ cytotoxic T cell line. The TCR transgenes were integrated into the genome of the B10.BR (H-2^k) mice (Geiger et al., 1992). Surprisingly, the heterozygous TG-B mice had high incidence of lymphoma regardless of sex. The maximal survival time for TG-B mice was 9 months with a median survival time of 6 months (Fig. 1A). The lymphoma in TG-B mice was first seen in lymphoid organs, including the thymus, spleen and lymph nodes (Fig. 1B). As the cancer progressed, the tumor cells infiltrated other organs, such as liver, kidney (Fig. 1C), lung, pancreas, intestines and salivary glands (data not shown). Further characterization of malignant cells revealed that the immunophenotype of the T cell lymphoma varied between animals suggesting that transformation occurred at various stages in T cell development (data not shown).

To test if the genetic background of mice affects tumor incidence, we produced the TG-BxC57BL/6 F1 mice and monitored their tumor incidence. Although T cell development in the F1 mice was normal (Zheng et al., 2002), significant reductions were observed in both incidence and onset in the F1 mice in comparison to the TG-B mice (Fig. 1A). This result demonstrates that the C57BL/6 mice had dominant genetic modifiers for the development of lymphoma, although close to 50% of the F1 mice still developed lymphoma within one year.

In order to understand the mechanism of tumorigenesis in these mice, we first determined the integration site of the transgene by fluorescence in situ hybridization (FISH)

using a biotin labelled DNA fragment probe from the TCR α chain constant region (Heng et al., 1992). DAPI banding was performed, and a strong signal was identified on one of the two chromosome 10 (Fig. 2A). The strong signal was localized to region 10A2 based on the summary of 10 images (data not shown). Two weaker FISH signals were detected, one on each copy of chromosome 14, consistent with the location of the endogenous TCRα genes. Fine mapping of integration sites was performed by the TOPO®Walker method (Shuman, 1994). PCR products using the TOPO®Linker primers and the gene specific sequence primers from both 3' and 5' termini of the TCR α and TCR β transgenes were cloned and sequenced. Three independent experiments revealed that the TCR α transgene was inserted into the intron 1 of EPM2a, which encodes laforin, a dual specific protein phosphatase (Fig. 2B) (Minassian et al., 1998; Serratosa et al., 1999b). Further PCR analysis using primers corresponding to the 3' terminus of the TCRα transgene and the 5' terminus of the TCRβ transgene confirmed that these genes were co-integrated into chromosome 10 in TG-B mice (Fig. 2C). The integration was confirmed by PCR using primers outside the sequence identified by the TOPO®Walker method (data not shown) and by Southern blot using the sequence adjacent to the integration site as probe (Fig. 2D). Additional chromosomal walking with the β-chain probe failed to identify other integration sites for the TCR β construct (Data not shown).

To determine whether the integration of the TCR transgene inhibited expression of the EPM2a gene, we examined the expression of the EPM2a gene in the thymi of nontransgenic (Ntg), transgenic littermates with no tumor (Tg) and transgenic mice that developed lymphoma (Tg-Tu). Based on RT-PCR amplification of full length transcript, EPM2a was expressed at significant levels in nontransgenic and transgenic littermates. However, its

expression in Tg-Tu lymphoma cells was greatly reduced (Fig. 3A). We analyzed *EPM2a*

gene product, laforin, by Western blot using a polyclonal antibody against laforin. We

showed that laforin was expressed in Tg mice with approximately half of the amount in NTg

mice, but was absent in the transgenic mice that developed lymphoma (Tg-Tu) (Fig. 3B).

This method also revealed the down-regulation of the laforin in the majority of the murine T

and B cell lymphoma cell lines that we tested (Fig. 3C). Thus, tumorigenesis was consistently

associated with altered laforin gene expression.

We have used PCR to distinguish the junction region of the transgenic and wild-type

alleles. Surprisingly, no homozygous mice were identified in over more than 60 offspring

tested, including both healthy and moribund mice. Further, preliminary analysis of embryos

from day 8 on also failed to identify a homozygous embryo. These data suggest that

homozygous integration causes early embryonic lethality. Interestingly, the high tumor

incidence and lack of laforin documented in Fig. 1A was observed in heterozygous mice.

Since the wild type allele was not deleted in the tumor cells lacking laforin expression (data

not shown), it may have been silenced by epigenetic mechanisms. The *EPM2a* gene contains

a 1.2 kb 5'-CpG island that spans the promoter region, exon 1 and part of intron 1 (Fig. 4A).

To determine if DNA hypermethylation is an epigenetic mechanism for laforin gene down-

regulation in TG-B lymphoma, we treated the genomic DNA with bisulfite and sequenced 4

PCR products covering 102 CpG di-nucleotides within the 5'-CpG island. Our preliminary

analyses of tumor samples indicated that a 333-bp fragment was the most frequently

methylated area (data not shown). We therefore focused on this region and examined six TG-

B mice that developed lymphoma and six TG-B mice that had not developed tumors. Based

on methylation-mediated protection of C>T conversion by the sodium bisulfite, we identified

the methylated CpG di-nucleotides. As illustrated in Fig. 4B, extensive hypermethylation was found in the *EPM2a* gene of all six lymphoma samples. In contrast, none of the normal thymi had methylation in this region. Our survey of multiple mouse lymphoma cell lines revealed that depression in the *EPM2a* gene was wide-spread among lymphomas (Fig. 3C). Moreover, treatment with methyl-transferase inhibitor 5-aza-2'-deoxycytidine increased *EPM2a* expression (Fig. 4C and data not shown). To test whether hypermethylation of the *EPM2a* promoter was responsible for repression of the *EPM2a* gene, we compared 3 non-lymphoid tumor cell lines with 3 T lymphoma cell lines for constitutive and 5-aza-2'-deoxycytidine-induced *EPM2a* expression. At the same time, *EPM2a* promoter hypermethylation was determined by quantitative real-time PCR based on susceptibility to a methylation-sensitive restriction enzyme. As shown in Fig. 4C, *EPM2a* was constitutively expressed at high levels in mastocytoma cell line P815, colon cancer cell line MC38 and fibrosarcoma Meth A. Treatment with 5-aza-2'-deoxycytidine had little effect on *EPM2a* expression in these 3 cell lines. The *EPM2a* promoter region in these three cell lines was not methylated as shown in Fig. 4D that the real time PCR failed to amplify the promoter region due to the methylation-sensitive restrictive enzyme *Sac* II activity that cut more than 99% of the *EPM2a* promoter. In contrast, in three T lymphoma cell lines tested, the *EPM2a* promoter region was completely resistant to *Sac* II enzyme activity and real time PCR successfully amplified the promoter region (Fig. 4D). Correspondingly, very little constitutive expression of *EPM2a* was found, and 5-aza-2'-deoxycytidine substantially induced *EPM2a* expression among the three T lymphoma cell lines, although the induction in the EL-4 cell line was less than in others (Fig. 4C). These data are consistent with the notion that hypermethylation is responsible for *EPM2a* down-regulation among T lymphomas.

The transgene expression may potentially activate genes in the area. There are two genes within 300kb to the transgene integration site. The proximal gene is 56 kb away from the integration site and encodes a protein that contains an F-box domain (mCG16603), while the other gene is 135 kb from the integration site (mCG140768) (Fig. S1A). We performed RNase protection assay to determine the mRNA expression of these two genes. The expression level of the distal gene (mCG140768) was not affected by transgene or lymphoma development, while the expression of the proximal gene (mCG16603) was up-regulated by the transgene regardless of lymphoma formation (Fig. S1B). We tested this possibility by producing 8 independent founders of transgenic mice that express mCG16603 under the control of a proximal *lck* promoter, which resulted in high levels of expression in the thymus. None of the mice developed lymphoma up to 22 months of observation (Fig. S1C). The offspring of one of the founders were observed over a one-year period. Although the mCG16603 is expressed at much higher level than in the TG-B mice (Fig. S1D), no lymphoma was observed in 12 mice observed over a 45-61 week period (Fig. S1C). Thus, the lymphoma development in TG-B mice is unlikely due to the abnormal expression of other genes near the integration site.

To test whether inactivation of the *EPM2a* gene is sufficient to cause abnormal cell growth, we tested the consequences of silencing the *EPM2a* gene in the bone marrow stem cells in both methylcellulose assay in vitro and bone marrow reconstitution in vivo. Unmanipulated murine bone marrow has a finite ability to serially replate in methylcellulose cultures supplemented with cytokines (Lavau et al., 1997). We constructed lentiviral vector expressing C-terminal siRNA for *EPM2a* or control sequence. Bone marrow cells from B10.BR mice pretreated with 5-fluorouracil (5-FU) were transduced with the siRNA or

control constructs and selected for blasticidin-resistant transduced cells in the first plating. Cells were cultured in vitro for four serial replatings and the number of colonies was counted under microscope. As shown in Fig. 5A, the number of colonies formed from 10^4 vector-transduced bone marrow cells steadily reduced over serial replating. In striking contrast, cells transduced with *EPM2a* siRNA had a drastic increase in the number of colonies in the third and fourth round, most of them tightly packed. These results demonstrated that silencing *EPM2a* drastically increased the self-renewel ability of the bone marrow stem cells.

To test whether silencing *EPM2a* in the bone marrow cells can cause hematological abnormality in vivo, we injected the siRNA transduced or control vector transduced P1CTL TCR-transgenic mouse bone marrow cells into irradiated syngeneic RAG-2 (-/-) mice. The mice were examined 4 months after the bone marrow reconstitution as the mice in the siRNA group started to loss weight and had difficulty in breathing. The random integration of viral constructs in bone marrow cells was confirmed by Southern blot (Fig. 5B). Examination of the bone marrow showed that in the chimera mice reconstituted with control vector transduced bone marrow, the myeloid over erythroid ratio was roughly 2:1, this ratio was drastically increased in 4 out of 5 recipients of siRNA-transduced bone marrow cells (P=0.004) (Fig. 5C). The increased M/E ratio was mainly due to the increase in mature and immature neutrophils and decreased erythroid cells in the bone marrow (Fig. 5D-a-b). In addition, we observed an increased cellularity of the bone marrow in the siRNA-transduced group (Fig. 5Da-b). The fifth recipient of siRNA-transduced bone marrow had about 50% of monocytes and monoblasts in the bone marrow (Fig. 5D-c) compared to less than 2% in control group (Fig. 5D-a), which is consistent with the diagnosis of chronic myelomonocytic leukemia. The cause of respiratory distress in the recipient mice that received siRNA transduced bone

marrow was due to a heavy infiltrate of monocytic cells and fibroblastic proliferation in the lung tissue (Fig. 5D-d and insert). These results, taken together, demonstrate that silencing of *EPM2a* resulted in myelodysplastic syndrome.

To test whether the hematological malignancy in the TG-B mice can be complemented by *EPM2a*, we generated *EPM2a* transgenic mice (FVB background) under the control of the *lck* promoter. Although the FVB background was less susceptible to lymphoma, about 40% of non-transgenic FVBxTG-B succumbed to lymphoma in one year. Complementation with the *EPM2a* transgene drastically decreased the incidence and delayed the onset of the lymphoma (Fig. 5E). Thus, *EPM2a* inactivation is both necessary and sufficient for the lymphoma that developed in the TG-B mice.

To test whether laforin can suppress the growth of other tumor cells, we transduced thymoma cell line BW5147 with either vector alone or *EPM2a*-containing lentiviral vectors. After a short-term drug selection, we compared vector and *EPM2a*-transfected tumor cells for their growth in vivo. As shown in Fig. 5F, the overexpression of laforin in *EPM2a*-transfectants had substantially reduced tumor growth in vivo. The tumor suppression depends on laforin's phosphatase activity, as inactivating mutation of the phosphatase (C265S) (Wang et al., 2002) abolished the tumor suppression. We also transfected the *EPM2a* cDNA into B104-1-1, a fibroblast cell line transformed by P185*neu* oncogene (Schechter et al., 1984). We inoculated the *EPM2a* or vector transfected B104-1-1 cell lines into *RAG-2(-/-)* mice that lacked T and B lymphocytes. Based on the kinetics of tumor growth, it was clear that overexpression of *EPM2a* had a significant suppressive effect on B104-1-1 tumor growth (Fig. 5G).

Laforin is the phosphatase for GSK3β

Because laforin suppressed growth of Her-2/Neu-transformed tumor cells, we explored

the possibility that laforin may be involved in PI-3K/Akt signaling pathway. Activation of the

platelet-derived growth factor (PDGF) receptor resulted in the recruitment of PI-3K isoforms

to the inner surface of the plasma membrane. This leds to activation of protein kinase B/Akt

(Romashkova and Makarov, 1999). We therefore transfected the *EPM2a* cDNA into NIH3T3

cells and evaluated the effect of laforin on platelet-derived growth factor (PDGF) receptor

signaling. We first examined phosphorylation of Akt at Thr 473 by 3'-phosphoinositide-

dependent protein kinase (PDK) (Alessi et al., 1997a). Activation and phosphorylation of

PDK was not significantly affected by PDGF in NIH3T3 cells, regardless of the expression of

laforin. As a result of PDK recruitment, significant Akt phosphorylation was observed

following PDGF stimulation, and again, this was only marginally affected by laforin

expression (Fig. 6A and Fig. S3). Interestingly, of the three down-stream targets of Akt

(Datta et al., 1999) that we examined, namely FKHR, AFX and GSK-3β, only GSK-3β

phosphorylation on Ser 9 was affected by over-expression of laforin (Fig. 6A). The effect was

highly selective as the phosphorylation of Tyr 216 of GSK-3β and Tyr 279 of GSK-3α was

not affected by laforin despite laforin's intrinsic dual specificity (Fig. 6B). To determine the

effect of laforin expression on GSK-3β activity, we precipitated GSK-3β and performed the in

vitro kinase assay to test its ability to phosphorylate recombinant protein Tau, a known GSK-

3β substrate (Cho and Johnson, 2003). As shown in Fig. 6C, PDGF-induced inhibition of

GSK-3β kinase activity was blocked in laforin-transfected cells. This was consistent with the effect of laforin on Akt-mediated phosphorylation of GSK-3β at Ser 9.

The selective effect of laforin on phosphorylation of GSK-3β at Ser 9 raised the intriguing possibility that laforin may be a missing phosphatase of GSK-3β. We took three approaches to substantiate this hypothesis. First, we generated the inhibitory siRNA expression construct and used this to eliminate the endogenous laforin in transfected NIH3T3 cells. Three C-terminal *EPM2a* siRNA stable transfectants were tested for transcriptional inhibition. As shown in Fig. 6D, *EPM2a* mRNA was reduced to levels undetectable by RT-PCR. Elimination of laforin expression had no effect on cellular levels of phospho-Akt, but as a result of siRNA inhibition of laforin, the phospho-GSK-3β became detectable even in the absence of PDGF. Furthermore, upon PDGF stimulation, levels of phospho-GSK-3β in cells treated with siRNA were higher than those found in vector-transfected control cells. SiRNA specific for another region of the *EPM2a* gene partially reduced laforin expression and lead to quantitative changes in GSK-3β phosphorylation (Supplemental Fig. S3A). The levels of GSK3β phosphorylation at Ser 9 correlated closely with the efficiency of laforin knockdown (Fig. S3A). In addition, the specificity of the knockdown is confirmed, as the biological effect was restored by reintroduction of human laforin, which had two basepair mismatch in the sequence targeted by the SiRNA (Supplemental Fig. S3B). Thus, laforin controls GSK-3β phosphorylation at Ser 9.

Secondly, we evaluated whether GSK-3β and laforin can physically associate with each other. We treated the vector and laforin-transfected NIH3T3 cells with PDGF and immunoprecipitated GSK-3β protein with either control IgG1 or a monoclonal anti-GSK-3β antibody. The precipitates were analyzed by Western blot with either anti-GSK-3β antibody or the anti-V5 antibodies that detect the V5-tagged laforin protein. As shown in Fig. 6E upper panel, anti-GSK-3β, but not control IgG1, brought down both GSK-3β and V5-tagged laforin

proteins in the *EPM2a*-transfected cells, but not in vector transfected cells. Thus, GSK-3β

and laforin are associated in the NIH3T3 cells. To determine whether GSK-3β associates

with endogenous laforin protein, we precipitated the GSK-3β in untransfected NIH3T3 cells

and probed the precipitates with antibody specific for laforin. As shown in Fig. 6E lower

panel, significant amounts of laforin was co-precipitated with GSK-3β. Thus, laforin

associates with GSK-3β under physiological condition. The association between GSK-3β and

laforin was independent of the phosphatase activity and was independent of stimulation by

PDGF (Supplemental Fig. S4).

As a third approach, we tested whether recombinant laforin can directly

dephosphorylate GSK-3β at Ser 9 in vitro. We purified wild-type or mutant laforin protein

with V5 tag from 293 transfectants by anti-V5 antibody coupled protein G beads. We used the

BSA-(bovine serum albumin) coupled synthetic N-terminal peptide of the GSK-3β with

phosphorylated Ser 9 as substrate. Ser 9-specific dephosphorylation was detected using

antibodies specific for the phosphorylated GSK-3β Ser 9. As shown in Fig. 6F, wild-type but

not the C265S mutant laforin dephosphorylated the p-Ser 9 peptide. The same laforin

preparation, however, failed to dephosphorylate Bad, which was phosphorylated *in vitro* by a

constitutively active recombinant Akt mutant protein (Fig. 6G). Recombinant laforin

expressed in bacteria showed similar specificity (Supplemental Fig. S5).

Laforin is an important modulator for Wnt signaling

GSK-3β is a major component in the Wnt signaling pathway (Cohen and Frame, 2001).

To understand how laforin may suppress tumor growth, we tested whether it may modulate

Wnt signaling. High dose of recombinant Wnt3A, when combined with low serum, induced

phosphorylation of GSK-3β. In addition, we found that Wnt-3A and PMA acted

synergistically to induce the phosphorylation of GSK-3β at Ser 9. The synergistic effect was

inhibited by an inhibitor of protein kinase C (Supplemental Fig. S6A). The PMA had no effect on phosphastase activity of laforin (Supplemental Fig. S6B). Neither Wnt3A nor PMA stimulation had any effect on the physical association between laforin and GSK-3β (Supplemental Fig. S6C). As such, we have used a suboptimal dose of PMA in conjunction with the Wnt3A. As shown in Fig. 7A, expression of laforin, but not the C265S mutant, decreased Ser 9 phosphorylation in GSK-3β upon Wnt-3A stimulation in conjunction with a suboptimal dose of PMA and decreased nuclear β-catenin accumulation. The functional importance of laforin expression in β-catenin activity was further confirmed by a TCF reporter assay (Korinek et al., 1997), as shown in Fig. 7B. Conversely, silencing the laforin expression in NIH3T3 cells significantly increased the phosphorylation of Ser 9 in GSK-3β and the nuclear accumulation of β-catenin upon high dose Wnt-3A stimulation (Fig. 7C).

To examine the relevance of laforin modulation of Wnt pathway in tumorigenesis, we evaluated GSK-3β phosphorylation and nuclear β-catenin accumulation in both laforin transfected tumor cell line and spontaneous lymphoma developed in TG-B mice that has a disrupted *EPM2a* gene. As shown in Fig. 7D, expression of laforin in B104-1-1 cells decreased the Ser 9 phosphorylation of GSK-3β and drastically decreased the nuclear accumulation of β-catenin, regardless of whether exogenous Wnt-3A was added. As shown in Fig. 7E, in transgenic mice that have one copy of the *EPM2a* inactivated, the thymocytes have a modest increase of phosphorylated GSK-3β in the cytosol, although no β-catenin was detected in the nuclei. In the lymphoma samples that had complete inactivation of the *EPM2a* gene, a drastic increase of GSK-3β phosphorylation and β-catenin accumulation in the nuclei were observed. These results demonstrate that laforin modulates Wnt signaling during tumorigenesis.

An interesting issue is whether the increased Wnt signalling is responsible for the tumorigenesis associated with *EPM2a* down-regulation. To test this possibility, we first used

16

the siRNA to silence *EPM2a* in a fibroblast cell line EEF8-TQ (Inoki et al., 2003) and injected the cells into immunodeficient host. As shown in Fig. 7F and supplemental Fig. S7, while the vector-transfected cells failed to produce tumors in the recipients, the *EPM2a*-silenced cells produced tumors in vivo. We then super-transfected the *EPM2a*-silenced cells with a dominant negative TCF1 (ΔTCF) to block the effector function of Wnt signaling. As shown in Fig. 7G, ΔTCF suppressed tumor growth induced by silencing *EPM2a*. These results demonstrate that laforin suppresses tumor growth by inhibiting Wnt signaling.

Discussion

By following a serendipitous observation of spontaneous lymphoma in a TCR transgenic mouse, we uncovered that laforin, a dual specific phosphatase with unknown function in signal transduction, is a key regulator for GSK-3β activity and suppresses tumor development and growth by modulating Wnt signaling.

Laforin is a tumor suppressor in the mouse

We have presented several lines of evidence that support a role for laforin as a tumor suppressor. First, we have identified by position cloning that a line of TCR transgenic mice with rapid onset and high penetrance of lymphoma has the transgene inserted in the intron 1 of the *EPM2a* gene. The insertion contains both α and β chains of genomic clone of a TCR and thus exceeds 100 kb (if one copy)-300 kb (if 3 copies as estimated by intensity of bands in Southern blot, data not shown). Since the heterozygous mice had roughly 50% of laforin protein expression, it is likely that such insertion inactivated the *EPM2a* locus. The development of lymphoma was associated with complete silencing of laforin gene, which in turn was due to hypermethylation of the *EPM2a* promoter. Thus, the genetic lesion and epigenetic inactivation of the *EPM2a* gene during tumorigenesis was reminiscent of a typical tumor suppressor gene (Paige, 2003). Second, we have demonstrated that hypermethylation of the *EPM2a* gene is not unique to the mouse lymphoma model in the TCR transgenic mice. Down-regulation of laforin is observed in a large panel of mouse lymphoma cell lines and correlates with hypermethylation of the locus. Thirdly, we have directly demonstrated the transgenic complementation of the *EPM2a* in T cell lineage prevented the development of T cell lymphoma in the TG-B mice. Conversely, suppression of *EPM2a* gene by siRNA increased tumorigenicity of a fibroblast cell line, promoted self-renewal ability of bone marrow hematopoietic stem cells, and caused myelodysplasia in vivo. Taken together, our data demonstrated that *EPM2a* inactivation is both necessary and sufficient for the

development of tumor in our mouse model. As such, the *EPM2a* gene is a tumor suppressor in the mouse model.

Several caveats deserve consideration.

First, mice with a targeted mutation of *EPM2a* gene have been reported to survive to 9 month of age, although it has not been examined as to whether the mice are more susceptible to lymphoma (Ganesh et al., 2002). It is therefore likely that the effect of targeted mutation in the mixed 129xC57BL/6 background (H-2^b) is less pronounced than what has been described here. This apparent inconsistency can be reconciled in two ways. The C57BL/6 (H-2^b) mice were less susceptible to lymphoma, as we showed that the TG-B(B10.BR, H-2^k) developed lymphoma substantially faster than the C57BL/6xTG-B F1. Likewise, the F1 between FVB (H-2^q) and TG-B also developed cancer at a reduced rate. In fact, the H-2 region has been shown to contain a major modifier for susceptibility to lymphoma (Kamoto et al., 1996). Nevertheless, it should be pointed out that the spontaneous tumor incidences in the two strains of F1 mice were still considerable. In addition, TCR transgenic mice are immune-deficient because their majority of their T cells were directed to a single CTL epitope and therefore unable to recognize tumor antigen. In support of the requirement for immunodeficiency, our analysis using siRNA-transduced bone marrow cells supported the importance of immunodeficiency, as hematological disorders were observed only when we used the bone marrow from TCR-transgenic mice to transplant to immunodeficient hosts. Other combinations that allowed reconstitution of immunity derived from either donor or host have been unsuccessful to induce malignancy (data not shown). The strain difference may also explain the fact that homozygous TG-B mice are embryonic lethal in B10.BR background while in the 129xC57BL/6 background, the *EPM2a* deficient mice are viable. In combination, these two factors can explain the lack of report on lymphoma in the *EPM2a*-deficient mice.

Second, insertion of TCR may cause aberrant expression of adjacent genes. We have found that the expression of one immediate neighbour (within 56 kb of *EPM2a*) was up-regulated, although no effect was observed on another gene 120 kb away. We have directly tested whether over-expression of the neighbouring gene was responsible for tumorigenesis by producing transgenic mice that over-express it in the thymus. Our analysis of 8 independent founders and the offspring of one of the founders revealed no lymphoma over more than 22 months-period. This result ruled out the possibility that over-expressing of the neighbouring gene was the primary event leading to cancer development. The tumor suppressor activity of *EPM2a* has been confirmed by *EPM2a* transgenic mice, by direct transfection and by siRNA knock-down experiments, in which the adjacent genes should not be affected.

Thirdly, it is of interest to consider whether *EPM2a* may be a tumor suppressor in human. Lafora's disease due to *EPM2a* mutation is a rare genetic disease with early lethality. The patients usually die before they reach 20 years of age. It is therefore difficult to evaluate the direct impact of this mutation on cancer incidence. In addition, *EPM2a* is located in 6q24 of human genome (Minassian et al., 1998; Serratosa et al., 1995; Serratosa et al., 1999b) where deletions or LOH were reported in cancers from a large number of different organs including carcinomas of the breast (Devilee et al., 1991; Sheng et al., 1996), endometrium (Tibiletti et al., 1997; Tibiletti et al., 1999), prostate (Cooney et al., 1996), lymphomas and leukemias (Gerard et al., 1997), and melanomas (Walker et al., 1994). Given the fact that the tumor phenotypes reported here has been observed in immune-deficient host, it is of particular interest to investigate the significance of *EPM2a* as a potential tumor suppressor gene in AIDS related malignancy, which is a growing medical problem. In this regard, it is worth noting that LOH in 6q24 is one of the most frequent chromosomal alterations in AIDS-related lymphoma (Gerard et al., 1997; Pastore et al., 1996; Zhang et al., 1997).

Laforin is the phosphatase for GSK-3β

GSK-3β is a key modulator for several important signal transduction pathways. Although GSK-3β is inactivated by phosphorylation at the Ser 9 position, it is unclear if the inactivated enzyme can be reactivated by dephosphorylation, as no specific phosphatase for this enzyme has been identified. Here we showed that laforin, a dual specific phosphatase with unknown substrate, is a specific phosphatase for GSK-3β. Thus, laforin is constitutively associated with GSK-3β in vivo and such association does not require its phosphatase activity. Recombinant laforin protein isolated from either eukaryotic or prokaryotic cells specifically dephosphorylated Ser 9 of GSK-3β but not unrelated Akt target, such as Bad. In vivo, transfection of laforin reduced PDGF-induced phosphorylation of Ser 9 of GSK-3β, but not that of Y216 of GSK-3β, Y279 of GSK-3α and the phosphorylation of PDK, Akt and other Akt substrates such as FKHR and AFX. Moreover, knockdown of laforin in either NIH3T3 cells or in TG-B mouse thymus substantially increased phosphorylation of GSK-3β. In addition, transfection of laforin substantially increased the enzymatic activity of GSK-3β. These data demonstrated that laforin is a critical regulator of Ser 9 phosphorylation and enzymatic activity of GSK-3β. Given the importance of GSK-3β in a variety of biological processes including cellular metabolism, growth and transformation, it would be of interest to determine which of these processes are also regulated by laforin.

Laforin as a critical modulator of Wnt signaling

We have taken two approaches to demonstrate that laforin is an important regulator in Wnt signalling. First, we showed that over-expression of laforin reduced nuclear

accumulation of β-catenin in response to Wnt3A. Conversely, knockdown of laforin in both cell lines and in transgenic mice resulted in a dose-dependent increase of β-catenin in the nuclei. Since nuclear accumulation of β-catenin play a major role in tumorigenesis, modulation of Wnt signaling is likely to be responsible for laforin-mediated suppression of tumor growth.

The detailed mechanism by which laforin regulate Wnt signaling has not been fully understood. Since we showed that laforin regulate Ser 9 phosphorylation of GSK-3β, a major regulator of β-catenin, the simplest hypothesis is that laforin modulate Wnt by regulating Ser 9 phosphorylation of GSK-3β and its biological activity. While our data are entirely consistent with this notion, three lines of evidence have questioned whether GSK-3β-mediated β-catenin destruction is regulated by phosphorylation of Ser 9. First, the GSK-3β in the Wnt pathway was thought to be insulated from the Akt pathway, partly because Wnt conditioned medium did not induce GSK-3β phosphorylation above the background (Ding et al., 2000). Second, genetic reconstitution in *Drosophila* demonstrated that the GSK-3β mutant that lacks Ser 9 can still mediate Wnt signaling (Papadopoulou et al., 2004). This later finding would argue that Ser 9 phosphorylation is not required for Wnt signalling in *Drosophila*. Interestingly, *Drosophila* also lacks the *EPM2a* gene (Ganesh et al., 2001). Thirdly, McManus et al. (McManus et al., 2005) reported recently that cells from the mice with knock-in of mutants GSK-3α (Ser21>Ala) and GSK-3β (Ser9>Ala) have the similar response to Wnt 3A as the wild-type control, which argued against an essential role for Ser 9 phosphorylation in Wnt signaling. On the other hand, LKB, which regulates Ser 9 phosphorylation by PKC was recently demonstrated to be an important regulator for Wnt signaling (Ossipova et al., 2003).

In this regard, we have observed that Wnt can synergize with PMA to induce Ser 9 phosphorylation of GSK-3β and that laforin is a potent regulator in this process. It is therefore possible that whether Ser 9 phosphorylation regulates Wnt signaling depends the context of Wnt signaling. Since the Wnt signaling complex is well insulated from the Akt pathway, Ser 9 phosphorylation may be important when PKC pathway is activated in the complex. These findings provide a plausible explanation for the need of GSK-3β-pocket that binds the priming site of the GSK-3β substrates (Amit et al., 2002; Liu et al., 2002; Yanagawa et al., 2002). Since development of tumors associated with *EPM2a* knockdown is completely inhibited by a dominant negative TCF mutation, *Epm2a*-mediated tumor suppression depends on its modulation of Wnt signaling.

Methods

Antibodies, phosphor-peptide, and recombinant proteins. Antibodies against the following proteins were used in this study: Akt, IκBα, β-catenin, phospho-Akt (Ser 473), phospho-GSK-3β (Ser 9), phospho-FKHR (Ser 256), phospho-PDK1 (Ser 241), phospho-GSK-3α/β(Ser 21/9) (Cell Signaling, Beverly, MA), GSK-3β (BD Pharmingen/Transduction Labs, San Diego, CA), V5 and anti-V5-HRP (Invitrogen Corp., Carlsbad, CA), p50, p65, Sp1, actin (I-19) (Santa Cruz Biotechnology, Inc. Santa Cruz, CA), and phospho-GSK-3α/β (pY 279/216) (Biosource International, Camarillo, CA). Other reagents were recombinant GSK-3β fusion protein and Akt1/PKB protein kinase (Cell Signaling), recombinant Tau protein (PanVera LLC, Madison, WI), human platelet-derived growth factor (PDGF) (Sigma, St. Louis, MO). BSA-coupled GSK3β phosphor-peptide were synthesized by Genemed Synthesis, Inc (San Francisco, CA). The peptide sequence is as follows: BSA-CGPKGPGRRGRRRTSS(phosphorylated)FAEG. Active Akt1/PKB protein kinase is a recombinant MBP-Akt1 fusion protein containing human Akt1 residues 140-480 with T308D, S473D mutations (Cell Signalling). Anti-Bad, anti-p-Bad (Ser 112) and recombinant full-length murine Bad fused with an N-terminal His 6-tag were purchased from Upstate (Lake Placid, NY).

Identification of transgene integration site. The fluorescence in situ hybridization (FISH) was performed by SeeDNA Biotech Inc. (Windsor, Ontario, Canada) using a 1.4 kb DNA fragment of TCR α chain constant region as the probe. The integration site of TCR transgene in chromosome 10 was identified using the TOPO®Walker Kit (Invitrogen) according to the protocol provided. Briefly, TCR transgenic mouse genomic DNA was digested by restrictive enzyme *Pst*I and dephosphorylated to allow ligation with the TOPO®Linker(Shuman, 1994). Primer extension using Taq polymerase and TCR specific primer 1 was performed to create double strand DNA that contained 3' A-overhangs. Dephosphorylated A-tailed DNA was

ligated with TOPO®Linker and further amplified by PCR. The PCR products were cloned into a TA-TOPO cloning vector (Invitrogen) and sequenced. The sequences were searched with the Celera Discovery System (Rockville, MD).

Bisulfite-PCR and sequencing. The methylation status of *EPM2A* was determined by bisulfite-PCR and sequencing. Bisulfite treatment was carried out as described previously (Clark et al., 1994). PCR was carried out with bisulfite-treated DNA as templates with 4 pairs of primers, LDM1.F. 5'-AGAGGTTTATAAAGGATTAAA TGTTGG, LDM1. R. 5'-TAAAATCAAAATTCCCAAAC (278bp); LDM2.F. 5'-GTTTGGGAATTTTGATTTTAC, LDM2.R. 5'-TAACCCGAATCCTAAAAACCTAAC (124bp); LDM3.F. 5'-GTTAGGTTTTTAGGATTYGGGTTAT, LDM3.R. 5'-CAATACCTTCCCAA TACAACTC (333bp); LDM4.F. 5'-GAGTTGTATTGGGAAGGTATTG, LDM4.R. 5'-AACTCTCCRAAATAAACCTAAAACC (222bp). The PCR products were purified by Gel Extraction kit (Qiagen), subcloned into the TA-TOPO vector system (Invitrogen) and sequenced by an ABI/PE 3700 capillary sequencer. 8-10 clones were sequenced for each lymphoma or normal thymus.

5-Aza-2'-deoxycitidine treatment. Cells were seeded at a density of 6×10^6 cells/10-cm plate and 5-Aza-dC (Sigma, St. Louis, MO) was added to different cell lines at maximal tolerable doses based on a 24-hour viability test (1 μM for P815, 2 μM for EL-4, RAW8.1 and S194, 3 μM for BW5147, CH27 and J558, 5 μM for RMA-S and A20, 10 μM for Yac-1, Meth A and Ag8.653, 20 μM for MC38). After 24 hrs, the medium was changed, and the cells were treated with fresh 5-Aza-dC for an additional 24 hrs. Two days after 5-Aza-dC treatment, the cells were harvested for RT-PCR analysis on *EPM2A* expression. Genomic DNA from three EPM2A high cell lines (P815, Meth A and MC38) and three EPM2A low lymphoma cell lines (EL-4, BW5147 and YAC-1) were subjected to methylation-sensitive *Sac* II digestion. Digested or undigested genomic DNA were used as templates for real time PCR.

Anti-laforin polyclonal antibody. The antibody was produced by Genemed Synthesis, Inc. (San Francisco, CA). Rabbits were immunized with the synthetic peptide of 16 amino acid residues (YKFLQREPGGELHWEG, residues 85–100 in laforin protein, Accession No. AAD26336) coupled with keyhole limpet hemocyanin (KLH) in complete Freund's adjuvant. The antiserum was purified using peptide conjugated Affigel column.

***EPM2A* siRNA constructs.** Oligonucleotides encoding siRNA directed against *EPM2a* at C terminal region of 934 to 954 nucleotides (5'-AAGGTGCAGTACTTCATCATG-3') (C) or polyA region of 1212 to 1233 nucleotides (5'-AAGGAAAACTGCATGCCACAT-3') (E) were subcloned into pSilencer 1.0-U6 siRNA expression vector (Ambion, Austin, TX) to generate C-siRNA according to manufacturer's protocol. NIH3T3 cells were co-transfected with C- or E-siRNA vector and pcDNA4/V5-His (Invitrogen) using Fugene 6 and selected by Zeocin. Individual clones were analyzed for *EPM2A* expression by RT-PCR. SiRNA sequence was also inserted into a modified pLenti6/V5-D-TOPO vector (Invitrogen). Lentivirus stocks were produced in 293FT cells according to manufacturer's protocol. Viral transduced cells were selected with blasticidin.

GSK-3β kinase assay. The *in vitro* kinase assay measuring the kinase activity of GSK-3β was performed according to a previously described protocol (Song et al., 2002).

Phosphatase assay. Fusion GSK-3β protein was phosphorylated in vitro with active Akt according to manufacturer's protocol (Cell Signalling). The *EPM2a* full length cDNA or its mutant C265S was cloned in pGEX-6P-1(Amersham) to create GST-Epm2a fusion protein. The soluble GST-fused protein was purified by glutathione-agarose beads, and eluted with 50mM reduced glutathione. Given concentrations of the laforin protein was mixed with the phosphorylated GSK-3β or with synthetic phospho-peptide of GSK-3β at serine9 in phosphatase assay buffer as described previously (Fernandez-Sanchez et al., 2003).

Cell fractionation and β-catenin analysis. Vector-, *EPM2A-* or siRNA-transfectants of

NIH3T3 or B104-1-1 cells were treated with or without recombinant mouse Wnt-3A protein

(500 ng/ml, R&D Systems, Minneapolis, MN) in DMEM medium containing 1% serum (high

dose condition, Fig. 7C and D), or Wnt3A (20 ng/ml) in conjunction of 0.5μM PMA (Fig. 7A)

for 3 hours. The cells were either directly lysed for the detection of p-GSK-3β levels in total

lysate or homogenized and fractioned for the detection of β-catenin levels in the nuclei in

Western blots.

TCF reporter assay. NIH3T3 transfectants in a 24-well plate were transfected with 0.2 μg of

pTOPFLASH or pFOPFLASH TCF luciferase reporter constructs (Cell Signalling) plus 0.05

μg of pRL-SV40 renilla luciferase control reporter. 24 hours later, the transfectants were

treated with Wnt-3A conditional medium or L-cell control medium for 16 hr. The luciferase

activity was determined by the Dual-luciferase reporter assay system (Promega, Madison,

WI). The results were shown after normalized to corresponding Renilla reporter value.

Methylcellulose bone marrow colony formation assay in vitro and bone marrow

reconstitution in vivo. Six to 8 weeks old mice were injected i.p. with 5-fluorouracil (150

mg/kg) five days prior to harvesting bone marrow cells from femurs. Concentrated lentiviral

supernatants were used to transduce bone marrow cells by a 2-hour spinoculation at 25 °C.

For methylcellulose colony assays, two days after infection, 1X10^4 of transduced B10.BR

bone marrow progenitor cells were plated in 0.9% methylcellulose (Stem cell Technologies,

Vancouver, BC, Canada) supplemented with 10 ng/ml of murine IL-3, IL-6, GM-CSF, 50

ng/ml SCF, and 3 u/ml hEpo (R&D systems, MN) in the presence of 5 μg/ml blastcidine.

After 7 days of culture, the number of colonies was counted and 1X10^4 cells of the single cell

suspensions prepared from blastcidine-resistant colonies were replated into methylcellulose

supplemented with the same growth factors without blastcidine. Further plating was repeated

every 10 days. To test the in vivo transformation, the vector or *EPM2a* siRNA-transduced

bone marrow cells from BALB/c.P1CTL (Sarma et al., 1999) (a TCR-transgenic strain

syngeneic to the RAG-2-/- recipient) were expanded in the medium containing above cytokine cocktail for 14 days. 5 μg/ml blastcidin was present during the third and fourth days. The expanded bone marrow cells were i.v. injected into sub-lethally irradiated RAG-2$^{-/-}$ mice (2x10^6/mouse). The mice were examined 4 months after the bone marrow reconstitution as the mice in the siRNA group started to loss weight and had difficulty in breathing.

Acknowledgements

References

Alessi, D. R., Deak, M., Casamayor, A., Caudwell, F. B., Morrice, N., Norman, D. G., Gaffney, P., Reese, C. B., MacDougall, C. N., Harbison, D., *et al.* (1997a). 3-Phosphoinositide-dependent protein kinase-1 (PDK1): structural and functional homology with the Drosophila DSTPK61 kinase. Curr Biol *7*, 776-789.

Alessi, D. R., and Downes, C. P. (1998). The role of PI 3-kinase in insulin action. Biochim Biophys Acta *1436*, 151-164.

Alessi, D. R., James, S. R., Downes, C. P., Holmes, A. B., Gaffney, P. R., Reese, C. B., and Cohen, P. (1997b). Characterization of a 3-phosphoinositide-dependent protein kinase which phosphorylates and activates protein kinase Balpha. Curr Biol *7*, 261-269.

Amit, S., Hatzubai, A., Birman, Y., Andersen, J. S., Ben-Shushan, E., Mann, M., Ben-Neriah, Y., and Alkalay, I. (2002). Axin-mediated CKI phosphorylation of beta-catenin at Ser 45: a molecular switch for the Wnt pathway. Genes Dev *16*, 1066-1076.

Behrens, J., von Kries, J. P., Kuhl, M., Bruhn, L., Wedlich, D., Grosschedl, R., and Birchmeier, W. (1996). Functional interaction of beta-catenin with the transcription factor LEF-1. Nature *382*, 638-642.

Bhanot, P., Brink, M., Samos, C. H., Hsieh, J. C., Wang, Y., Macke, J. P., Andrew, D., Nathans, J., and Nusse, R. (1996). A new member of the frizzled family from Drosophila functions as a Wingless receptor. Nature *382*, 225-230.

Cho, J. H., and Johnson, G. V. (2003). Glycogen synthase kinase 3beta phosphorylates tau at both primed and unprimed sites. Differential impact on microtubule binding. J Biol Chem *278*, 187-193.

Clark, S. J., Harrison, J., Paul, C. L., and Frommer, M. (1994). High sensitivity mapping of methylated cytosines. Nucleic Acids Res *22*, 2990-2997.

Cohen, P., and Frame, S. (2001). The renaissance of GSK3. Nat Rev Mol Cell Biol *2*, 769-776.

Cooney, K. A., Wetzel, J. C., Consolino, C. M., and Wojno, K. J. (1996). Identification and characterization of proximal 6q deletions in prostate cancer. Cancer Res *56*, 4150-4153.

Cross, D. A., Alessi, D. R., Cohen, P., Andjelkovich, M., and Hemmings, B. A. (1995). Inhibition of glycogen synthase kinase-3 by insulin mediated by protein kinase B. Nature *378*, 785-789.

Dajani, R., Fraser, E., Roe, S. M., Young, N., Good, V., Dale, T. C., and Pearl, L. H. (2001). Crystal structure of glycogen synthase kinase 3 beta: structural basis for phosphate-primed substrate specificity and autoinhibition. Cell *105*, 721-732.

Datta, S. R., Brunet, A., and Greenberg, M. E. (1999). Cellular survival: a play in three Akts. Genes Dev *13*, 2905-2927.

Devilee, P., van Vliet, M., van Sloun, P., Kuipers Dijkshoorn, N., Hermans, J., Pearson, P. L., and Cornelisse, C. J. (1991). Allelotype of human breast carcinoma: a second major site for loss of heterozygosity is on chromosome 6q. Oncogene *6*, 1705-1711.

Ding, V. W., Chen, R. H., and McCormick, F. (2000). Differential regulation of glycogen synthase kinase 3beta by insulin and Wnt signaling. J Biol Chem *275*, 32475-32481.

Doble, B. W., and Woodgett, J. R. (2003). GSK-3: tricks of the trade for a multi-tasking kinase. J Cell Sci *116*, 1175-1186.

Fernandez-Sanchez, M. E., Criado-Garcia, O., Heath, K. E., Garcia-Fojeda, B., Medrano-Fernandez, I., Gomez-Garre, P., Sanz, P., Serratosa, J. M., and Rodriguez de Cordoba, S. (2003). Laforin, the dual-phosphatase responsible for Lafora disease, interacts with R5 (PTG), a regulatory subunit of protein phosphatase-1 that enhances glycogen accumulation. Hum Mol Genet *12*, 3161-3171.

Frame, S., and Cohen, P. (2001). GSK3 takes centre stage more than 20 years after its discovery. Biochem J *359*, 1-16.

Frame, S., Cohen, P., and Biondi, R. M. (2001). A common phosphate binding site explains the unique substrate specificity of GSK3 and its inactivation by phosphorylation. Mol Cell *7*, 1321-1327.

Ganesh, S., Agarwala, K. L., Amano, K., Suzuki, T., Delgado-Escueta, A. V., and Yamakawa, K. (2001). Regional and developmental expression of Epm2a gene and its evolutionary conservation. Biochem Biophys Res Commun *283*, 1046-1053.

Ganesh, S., Delgado-Escueta, A. V., Sakamoto, T., Avila, M. R., Machado-Salas, J., Hoshii, Y., Akagi, T., Gomi, H., Suzuki, T., Amano, K., *et al.* (2002). Targeted disruption of the Epm2a gene causes formation of Lafora inclusion bodies, neurodegeneration, ataxia, myoclonus epilepsy and impaired behavioral response in mice. Hum Mol Genet *11*, 1251-1262.

Geiger, T., Gooding, L. R., and Flavell, R. A. (1992). T-cell responsiveness to an oncogenic peripheral protein and spontaneous autoimmunity in transgenic mice. Proc Natl Acad Sci U S A *89*, 2985-2989.

Gerard, B., Cave, H., Guidal, C., Dastugue, N., Vilmer, E., and Grandchamp, B. (1997). Delineation of a 6 cM commonly deleted region in childhood acute lymphoblastic leukemia on the 6q chromosomal arm. Leukemia *11*, 228-232.

Hagen, T., Di Daniel, E., Culbert, A. A., and Reith, A. D. (2002). Expression and characterization of GSK-3 mutants and their effect on beta-catenin phosphorylation in intact cells. J Biol Chem *277*, 23330-23335.

He, X., Saint-Jeannet, J. P., Wang, Y., Nathans, J., Dawid, I., and Varmus, H. (1997). A member of the Frizzled protein family mediating axis induction by Wnt-5A. Science *275*, 1652-1654.

Heng, H. H., Squire, J., and Tsui, L. C. (1992). High-resolution mapping of mammalian genes by in situ hybridization to free chromatin. Proc Natl Acad Sci U S A *89*, 9509-9513.

Ikeda, S., Kishida, S., Yamamoto, H., Murai, H., Koyama, S., and Kikuchi, A. (1998). Axin, a negative regulator of the Wnt signaling pathway, forms a complex with GSK-3beta and beta-catenin and promotes GSK-3beta- dependent phosphorylation of beta-catenin. Embo J *17*, 1371-1384.

Inoki, K., Zhu, T., and Guan, K. L. (2003). TSC2 mediates cellular energy response to control cell growth and survival. Cell *115*, 577-590.

Kamoto, T., Shisa, H., Pataer, A., Lu, L., Yoshida, O., Yamada, Y., and Hiai, H. (1996). A quantitative trait locus in major histocompatibility complex determining latent period of mouse lymphomas. Jpn J Cancer Res *87*, 401-404.

Korinek, V., Barker, N., Morin, P. J., van Wichen, D., de Weger, R., Kinzler, K. W., Vogelstein, B., and Clevers, H. (1997). Constitutive transcriptional activation by a beta-catenin-Tcf complex in APC-/- colon carcinoma. Science *275*, 1784-1787.

Lavau, C., Szilvassy, S. J., Slany, R., and Cleary, M. L. (1997). Immortalization and leukemic transformation of a myelomonocytic precursor by retrovirally transduced HRX-ENL. Embo J *16*, 4226-4237.

Liu, C., Li, Y., Semenov, M., Han, C., Baeg, G. H., Tan, Y., Zhang, Z., Lin, X., and He, X. (2002). Control of beta-catenin phosphorylation/degradation by a dual-kinase mechanism. Cell *108*, 837-847.

Manoukian, A. S., and Woodgett, J. R. (2002). Role of glycogen synthase kinase-3 in cancer: regulation by Wnts and other signaling pathways. Adv Cancer Res *84*, 203-229.

McManus, E. J., Sakamoto, K., Armit, L. J., Ronaldson, L., Shpiro, N., Marquez, R., and Alessi, D. R. (2005). Role that phosphorylation of GSK3 plays in insulin and Wnt signalling defined by knockin analysis. Embo J *24*, 1571-1583.

Miller, J. R. (2002). The Wnts. Genome Biol *3*, REVIEWS3001.

Minassian, B. A. (2001). Lafora's disease: towards a clinical, pathologic, and molecular synthesis. Pediatr Neurol *25*, 21-29.

Minassian, B. A. (2002). Progressive myoclonus epilepsy with polyglucosan bodies: Lafora disease. Adv Neurol *89*, 199-210.

Minassian, B. A., Lee, J. R., Herbrick, J. A., Huizenga, J., Soder, S., Mungall, A. J., Dunham, I., Gardner, R., Fong, C. Y., Carpenter, S., *et al.* (1998). Mutations in a gene encoding a novel protein tyrosine phosphatase cause progressive myoclonus epilepsy. Nat Genet *20*, 171-174.

Molenaar, M., van de Wetering, M., Oosterwegel, M., Peterson-Maduro, J., Godsave, S., Korinek, V., Roose, J., Destree, O., and Clevers, H. (1996). XTcf-3 transcription factor mediates beta-catenin-induced axis formation in Xenopus embryos. Cell *86*, 391-399.

Ossipova, O., Bardeesy, N., DePinho, R. A., and Green, J. B. (2003). LKB1 (XEEK1) regulates Wnt signalling in vertebrate development. Nat Cell Biol *5*, 889-894.

Paige, A. J. (2003). Redefining tumour suppressor genes: exceptions to the two-hit hypothesis. Cell Mol Life Sci *60*, 2147-2163.

Papadopoulou, D., Bianchi, M. W., and Bourouis, M. (2004). Functional studies of shaggy/glycogen synthase kinase 3 phosphorylation sites in Drosophila melanogaster. Mol Cell Biol *24*, 4909-4919.

Pastore, C., Carbone, A., Gloghini, A., Volpe, G., Saglio, G., and Gaidano, G. (1996). Association of 6q deletions with AIDS-related diffuse large cell lymphoma. Leukemia *10*, 1051-1053.

Peifer, M., and Polakis, P. (2000). Wnt signaling in oncogenesis and embryogenesis--a look outside the nucleus. Science *287*, 1606-1609.

Polakis, P. (2000). Wnt signaling and cancer. Genes Dev *14*, 1837-1851.

Reimann, J., Rudolphi, A., Tcherepnev, G., Skov, S., and Claesson, M. H. (1994). TCR/CD3 ligation of a TCR-transgenic T lymphoma blocks its proliferation in vitro but does not affect its growth in vivo. Exp Clin Immunogenet *11*, 197-208.

Romashkova, J. A., and Makarov, S. S. (1999). NF-kappaB is a target of AKT in anti-apoptotic PDGF signalling. Nature *401*, 86-90.

Sarma, S., Guo, Y., Guilloux, Y., Lee, C., Bai, X.-F., and Liu, Y. (1999). Cytotoxic T lymphocytes to an unmutated tumor antigen P1A: normal development but restrained effector function. J Exp Med *189*, 811-820.

Schechter, A. L., Stern, D. F., Vaidyanathan, L., Decker, S. J., Drebin, J. A., Greene, M. I., and Weinberg, R. A. (1984). The neu oncogene: an erb-B-related gene encoding a 185,000-Mr tumour antigen. Nature *312*, 513-516.

Serratosa, J. M., Delgado-Escueta, A. V., Posada, I., Shih, S., Drury, I., Berciano, J., Zabala, J. A., Antunez, M. C., and Sparkes, R. S. (1995). The gene for progressive myoclonus epilepsy of the Lafora type maps to chromosome 6q. Hum Mol Genet *4*, 1657-1663.

Serratosa, J. M., Gardiner, R. M., Lehesjoki, A. E., Pennacchio, L. A., and Myers, R. M. (1999a). The molecular genetic bases of the progressive myoclonus epilepsies. Adv Neurol *79*, 383-398.

Serratosa, J. M., Gomez-Garre, P., Gallardo, M. E., Anta, B., de Bernabe, D. B., Lindhout, D., Augustijn, P. B., Tassinari, C. A., Malafosse, R. M., Topcu, M., *et al.* (1999b). A novel protein tyrosine phosphatase gene is mutated in progressive myoclonus epilepsy of the Lafora type (EPM2). Hum Mol Genet *8*, 345-352.

Sheng, Z. M., Marchetti, A., Buttitta, F., Champeme, M. H., Campani, D., Bistocchi, M., Lidereau, R., and Callahan, R. (1996). Multiple regions of chromosome 6q affected by loss of heterozygosity in primary human breast carcinomas. Br J Cancer *73*, 144-147.

Shuman, S. (1994). Novel approach to molecular cloning and polynucleotide synthesis using vaccinia DNA topoisomerase. J Biol Chem *269*, 32678-32684.

Song, L., De Sarno, P., and Jope, R. S. (2002). Central role of glycogen synthase kinase-3beta in endoplasmic reticulum stress-induced caspase-3 activation. J Biol Chem *277*, 44701-44708.

Tibiletti, M. G., Bernasconi, B., Taborelli, M., Furlan, D., Fabbri, A., Franchi, M., Taramelli, R., Trubia, M., and Capella, C. (1997). Involvement of chromosome 6 in endometrial cancer. Br J Cancer *75*, 1831-1835.

Tibiletti, M. G., Furlan, D., Taborelli, M., Facco, C., Riva, C., Franchi, M., Cossu, A., Trubia, M., Taramelli, R., and Capella, C. (1999). Microsatellite instability in endometrial cancer: relation to histological subtypes. Gynecol Oncol *73*, 247-252.

Walker, G. J., Palmer, J. M., Walters, M. K., Nancarrow, D. J., Parsons, P. G., and Hayward, N. K. (1994). Simple tandem repeat allelic deletions confirm the preferential loss of distal chromosome 6q in melanoma. Int J Cancer *58*, 203-206.

Wang, J., Stuckey, J. A., Wishart, M. J., and Dixon, J. E. (2002). A unique carbohydrate binding domain targets the lafora disease phosphatase to glycogen. J Biol Chem *277*, 2377-2380.

Woodgett, J. R. (2001). Judging a protein by more than its name: GSK-3. Sci STKE *2001*, RE12.

Yanagawa, S., Matsuda, Y., Lee, J. S., Matsubayashi, H., Sese, S., Kadowaki, T., and Ishimoto, A. (2002). Casein kinase I phosphorylates the Armadillo protein and induces its degradation in Drosophila. Embo J *21*, 1733-1742.

Zeng, L., Fagotto, F., Zhang, T., Hsu, W., Vasicek, T. J., Perry, W. L., 3rd, Lee, J. J., Tilghman, S. M., Gumbiner, B. M., and Costantini, F. (1997). The mouse Fused locus encodes Axin, an inhibitor of the Wnt signaling pathway that regulates embryonic axis formation. Cell *90*, 181-192.

Zhang, Y., Weber-Matthiesen, K., Siebert, R., Matthiesen, P., and Schlegelberger, B. (1997). Frequent deletions of 6q23-24 in B-cell non-Hodgkin's lymphomas detected by fluorescence in situ hybridization. Genes Chromosomes Cancer *18*, 310-313.

Zheng, X., Gao, J. X., Zhang, H., Geiger, T. L., Liu, Y., and Zheng, P. (2002). Clonal deletion of simian virus 40 large T antigen-specific T cells in the transgenic adenocarcinoma of mouse prostate mice: an important role for clonal deletion in shaping the repertoire of T cells specific for antigens overexpressed in solid tumors. J Immunol *169*, 4761-4769.

Figure legends

Fig. 1. A transgenic mouse (TG-B) line with high penetrance, early lethality lymphoma. The transgenes, the re-arranged α and β chain genes of the T cell receptor, were obtained from a $CD8^+$ T cell clone with specificity for SV40 large T antigen. Since its generation, the transgenic mice have been backcrossed to B10.BR background for more than 30 generations. A. The survival distribution function among B10.BR (n=50), TG-B (n=62) and F1 (TG-B x C57BL/6) (n=30) mice. The incidence of lymphoma is significantly higher among TG-B in comparison to WT (P<0.0001) and F1 (TG-B x B6) mice (P<0.0001). F1 (TG-B x B6) mice developed lymphoma at a significant higher rate in comparison to WT mice (P<0.0001). B. Enlargement of spleen (top), thymus (middle) and mesenteric lymph node (MLN, bottom) in a TG-B mouse with tumor (left panels), organs from a TG-B mouse that have not developed tumor are shown as controls. C. Immunohistochemical staining of anti-Thy1 in non-Tg spleen (a) showing normal T cell distribution and in speen from TG-B mouse with lymphoma (b) showing the entire spleen was infiltrated by large lymphoblastic T cells. H&E sections of liver (c) and kidney (d) of the tumor-bearing TG-B mice showing the infiltration of lymphoma cells in organs.

Fig. 2. Identification of the integration site of the TCR transgene. A. Cytogenetic analysis of TCR gene localization by FISH. The probe used was the constant region of the TCR α chain. The location of the transgene is indicated by an arrow in the left panel, the positions of chromosomes 10 and 14 are marked in the right panel. The signals in chromosome 14 reflect the location of the endogenous TCR α loci. The signal in chromosome 10 is the transgene insertion locus. B. Identification of the TCR integration site by PCR-based TOPO®Walker

method using the TOPO®Linker primers and the gene specific sequence primers from both 3'
and 5' termini of the TCR α and TCR β transgenes. The primer that corresponded to 3'
terminus of the TCRα-chain yielded PCR products with TCR gene sequence. Junction
sequence of TCRCα and chromosome 10 DNA is shown. This is extracted from sequence of
4 clones. C. Chromatogram depicting the junctional sequence of TCRα and β constructs. D.
Confirmation of the integration site by Southern blot. The restriction enzyme map of
endogenous and Tg alleles and a Southern blot autograph are shown. E. A portion of the
10A2 region in relation to the integration site is indicated. Note that the integration site is in
intron 1 of *EPM2a*, which encodes for laforin.

Fig. 3. Defective expression of laforin in lymphoma. A. Defective expression of *EPM2a*
mRNA in transgenic mice with lymphoma (Tg-Tu), but not in the non-transgenic littermates
(Ntg), or in young transgenic mice that have not yet developed lymphoma (Tg). Total RNA
was isolated from thymi. The cDNA was prepared by reverse transcription and amplified
using primers that amplify the entire coding sequence of *EPM2a*. B. Absence of laforin
protein expression in Tg-Tu lymphoma cells and reduction of laforin expression in young
transgenic (Tg) thymocytes, as analyzed by Western blot using a polyclonal anti-laforin
antibody. C. Down-regulation of laforin protein in multiple murine malignancies of T, B cell
lineages. The thymocytes from a non-transgenic littermate (Ntg) and two transgenic mice with
lymphoma (Tg-Tu) were examined as control. The malignant cell lines used were T cell
lymphoma EL4, YAC-1, BW5147 and RMA-S, B cell lymphoma A20, RAW8.1, CH27,
myeloma S194. Data shown are representative of three independent experiments.

Fig. 4. *EPM2a* is hypermethylated in lymphoma cells. A. Diagram of 5'-CpG island and the location of the 4 primer sets used to amplify the bisulfite treated DNA to examine the methylation status of the *EPM2a* gene. The 5'-CpG island was 1225 bp in length with 59.2% GC content. The ratio of observed CpG to expected CpG is 0.948. The length of PCR products and the number of CpG di-nucleotides (in parentheses) within each PCR products are labelled. B. Summary of the results of bisulfite sequencing of PCR products with LDM3 which contained 45 CpG di-nucleotides. Fifty seven clones were obtained from six lymphoma mice (clone numbers from each mouse are labelled in parentheses) and 45 clones were obtained from six transgenic littermates without lymphoma (10 each from three mice, and 15 clones from a pool of three mouse thymi). Each circle represents the methylation status of a CpG di-nucleotide from 8-10 clones, except the last line of circles from which each circle represents results from 15 clones. Methylated and unmethylated alleles are shown as solid and open circles, respectively. C. 5-AzaC–induced *EPM2a* expression in lymphoma cell lines, but not in 3 non-lymphoid tumor cell lines. Cells were collected after 48 hr of treatment with or without 5-aza-2'-deoxycytidine. Total RNA was isolated and RT-PCR was done using primers that amplified the entire coding sequence of *EPM2a*. The cell lines used were T cell lymphoma EL4, YAC-1 and BW5147, mastocytoma P815, colon cancer MC38 and fibrosarcoma Meth A. D. DNA methylation in lymphoma cell lines. Genomic DNA from the cell lines were isolated and treated with or without methylation-sensitive restrictive enzyme *Sac* II overnight. The 280 bp promoter was amplified by real-time PCR. To normalize against DNA loss associated with enzyme digestion and purification, the difference between *Sac* II-treated and untreated samples with 0% methylation (as determined by bisulfate

sequencing, mouse No. 11992) was subtracted from all digested samples. DNA from a TG-B thymoma (No. 4012) with 100% methylation was used as positive control.

Fig. 5. *In vitro* and *in vivo* transformation of bone marrow stem cells by silencing *EPM2a*. A. Silencing *EPM2a* greatly increased self-renewal of bone marrow hematopoietic stem cells. B10.BR mice were pretreated with 5' FU and bone marrow cells were isolated and transduced with lentiviral vectors with either stuffer sequenece (vector) or that encodes the C-terminal siRNA of *EPM2a*. The transduced bone marrow cells (10^4/well) were serially replated four rounds in methylcellulose and blasticidin was added in first round. Data shown are means +/- SD of colony numbers in triplicate plates, and are representative of 3 independent experiments. B-D, Hematological disorders associated with silencing *EPM2a*. Bone marrow cells from 5'FU-pretreated P1CTL TCR-transgenic mice (BALB/c background) were transduced with either lentiviral vector or those that encode SiRNA. After 2-day blastcidin selection, the transduced cells were expanded in the presence of growth factors for two weeks and transferred into sub-lethally irradiated immunodeficient BALB/c.*RAG-2*$^{-/-}$ hosts. Four months later, when the recipients of the *Epm2a* silenced mice become moribund, the chimera mice from both groups were sacrificed for analysis. B. Bone marrow Southern blot using blasticidin resistant gene as probe showing random integration of the lentiviral vector in the recipients of the *EPM2a*-silenced bone marrow. Note the distinct pattern of individual mouse. C. Bone marrow cell counting showing different myeloid/erythroid (M/E) ratio in the recipients of the vector-transduced (n=6) or SiRNA-transduced (n=4) bone marrow cells (P=0.004). The fifth case with a different presentation was not included. D. H&E staining of bone marrow sections from the recipients of the vector-transduced (D-a) or SiRNA-transduced (D-b) bone marrow cells. D-a represents the histology of 6 vector-transduced

bone marrow (50x objective), while D-b represents 4/5 of SiRNA-transduced bone marrow (50x objective). Note increase of cellularity and the M/E ratio in b, which is mostly due to increase in mature and immature neutrophils. D-c represents the histology of the fifth recipient of siRNA-transduced bone marrow showing greatly increased (46%) and clustered monocytes and monoblasts (yellow dotted circle) which contained indented and lobulated nuclei that had 1-3 conspicuous nucleoli per nucleus (50x objective). D-d represents massive pulmonary infiltration and consolidation in lung tissues that completely obliterated the pulmonary parenchyma from recipients of siRNA-transduced bone marrow (10x objective). The insert showing the homogeneous infiltrating cells with abundant cytoplasm and large indented and lobulated nuclei that had 1-3 conspicuous nucleoli per nucleus (50x objective) Similar histological features were observed in 3/5 siRNA-transduced bone marrow recipients, but not in any of the 6 vector-transduced bone marrow recipients. E. *EPM2a* complementation suppresses tumorigenesis associated with the TG-B mice. *EPM2a* cDNA were inserted into transgenic vector with approximal *lck* promoter. Founder mice with ectopic expression of *EPM2a* were crossed with the TG-B mice. The survival of the $EPM2a^+$ TG-B (n=26) and $EPM2a^-$ TG-B (n=33) littermates were observed over a 70 week period (P=0.02). Moribund mice were sacrificed to confirm development of lymphoma. The insert showed the expression of *EPM2a* in $EPM2a^+$ and $EPM2a^-$ thymocytes as determined by RT-PCR. F. Laforin suppresses the growth of murine T cell lymphoma BW5147. BW5147 cells were transfected with vector only or with either wild-type or C265S mutant *EPM2A* cDNAs. Polyclonal stable transfectants were injected subcutaneously into the RAG-2(-/-) BALB/c mice (3 x 10^5 cells/mouse). The growth kinetics was presented. The expression of the V5-tagged and the minute amounts of endogenous laforin is shown in the insert. G. Laforin

suppresses the growth of P185neu-transformed NIH3T3 cell line B104-1-1. B104-1-1 cells were transfected with either vector or *EPM2A* cDNA. Three stable clones from each group (Vector or Laforin) were injected into the RAG-2(-/-) BALB/c mice ($3x10^5$ cells/mouse). The growth kinetics was presented. Data shown are representative of two independent experiments. The expression of the V5-tagged and the minute amounts of endogenous Laforin is shown underneath.

Fig. 6. Laforin is a phosphatase of GSK-3β at Ser 9. A. Laforin selectively prevented PDGF-induced phosphorylation of GSK-3β. Vector or laforin-V5 transfected NIH3T3 cells were stimulated with PDGF for given periods of time. The activation of PDK (anti-phosphorylated Ser241), Akt (anti-phosphorylated Ser473), GSK-3β (anti-phosphorylated Ser9), FKHR (anti-phosphorylated Ser256), and AFX(anti-phosphorylated Ser193) were analyzed by Western blot. Amounts of protein loaded were revealed using the total Akt as determined by Western blot. B. Laforin dephosphorylated the phospho-Ser 9, but not P-tyrosine 216 of GSK-3β and P-tyrosine 279 of GSK-3α. Two stable laforin transfected clones are presented (D2 and D7). C. Laforin prevented PDGF induced inactivation of GSK-3β kinase activity. Vector or laforin-transfected NIH3T3 cells were stimulated with PDGF for 30 minutes and the cells were lysed and subjected to immunoprecipitation with anti-GSK-3β antibody. The immunoprecipitates were used for kinase assay to determine the GSK-3β kinase activity. Recombinant Tau protein and ^{32}P-γ-ATP were used as substrates. Specific phosphorylation of Tau was determined by ^{32}P autoradiograph. The GSK-3β in immunoprecipitates was determined by Western blot with anti-GSK-3β. The radioactive intensity in each lane was normalized based on the amounts of GSK-3β in each sample, as determined by Western blot.

In order to compare different experiments, we arbitrarily assigned the activity of the GSK-3β isolated from untreated vector-transfectants as 1.0. Statistical difference was calculated by student t-tests. Data shown are summary of 3 independent experiments. D. siRNA suppresses endogenous laforin and enhances the PDGF induced phosphorylation of GSK-3β. Oligonucleotides encoding siRNA against the C-termini of *Epm2a* was subcloned into pSilencer™ 1.0-U6 siRNA expression vector (Ambion). The upper panel shows the efficiency of endogenous *EPM2a* suppression in three stable clones C1, C2 and C3 by RT-PCR. The activation of Akt (anti-phosphorylated Ser473) and GSK-3β (anti-phosphorylated Ser 9) from vector or siRNA C3 transfected NIH3T3 cells were analyzed by Western blot. β-actin was the protein loading control. E. Physical association between GSK-3β and laforin. Upper panel shows association of transfected laforin with GSK-3β. Vector or laforin-transfected NIH3T3 cells were stimulated with PDGF for 30 min and cell lysates were immunoprecipitated with either control IgG1 or anti- GSK-3β monoclonal antibody. The precipitates were then blotted with either anti- GSK-3β or anti-V5 antibodies to detect the V5-tagged laforin protein. The lower panel shows association between GSK-3β and laforin in untransfected 3T3 cells. As in the upper panel, except that the cells were untransfected and the Laforin were probed with anti-Laforin antibody. F&G. Laforin dephosphorylates P-Ser9 of GSK-3β (F) but not PSer112 of BAD in vitro (G). P-Ser9-phosphorylated peptide of GSK-3β was conjugated in bovine serum albumin (BSA) and recombinant soluble Bad protein was phosphorylated by constitutively activated Akt in the presence of ATP. The wild type or mutant of *EPM2a* was transiently transfected into HEK293 and immunoprecipitated with anti-V5 monoclonal antibody after 48 hours transfection. An aliquot of the precipitates was added to the mixture of either serine 9 phosphorylated peptide of GSK-3β or AKT-phosphorylated Bad. After 30 min

incubation at 37° C, loading buffer was used to terminate the reaction and was loaded to 10%

SDS-PAGE for Western blot using antibody of either anti-phospho-GSK-3β (Ser9) or anti-

phospho-Bad (Ser112). After that, the membrane was stripped for detecting Laforin-V5 (F

middle panel, G lower panel) or Bad (G middle panel). The protein composition of the

precipitates was analyzed by SDS-PAGE and detected by Coomassie blue staining (F lower

panel). Data shown represent at least three independent experiments.

Fig. 7. Laforin modulates Wnt signalling pathway. A. Vector (V), laforin (D2, D7, D14) or

mutant (C265S)-transfected NIH3T3 cells were stimulated with recombinant Wnt-3A (20

ng/ml) plus PMA (0.5 μM). At 3 hours after stimulation, the cell lysates were analyzed for

phosphorylation of GSK-3β at Ser 9 by Western blot. Protein loading is indicated by blotting

with anti-GSK-3β antibody. The nuclear fractions were isolated to determine the amounts of

β-catenin. Protein loadings in the nuclear fractions were indicated by anti-SP1 blot. B. TCF

reporter assay. pTOPFLASH or pFOPFLASH TCF luciferase reporter vector was co-

transfected with pRL-SV40 Ranilla control luciferase reporter plasmid into Vector (V), laforin

(D14) or mutant laforin (C265S) stably transfected NIH3T3 cells. Twenty four hours after

transfection, the cells were stimulated with Wnt-3A conditional medium or control medium

overnight. Cell lysate supernatants were evaluated for luciferase activity by Dual-luciferase

reporter assay system. The results are shown after normalized to corresponding Renilla

reporter value. C. Silencing siRNA increased the GSK-3β-phosphorylation, and β-catenin

nuclear accumulation by Wnt-3A. Vector (V) or C-terminal silencing siRNA (C3) transfected

NIH3T3 cells were stimulated by high dose (500 ng/ml) recombinant Wnt-3A. Phospho-Ser 9

GSK-3β in cell lysate and β-catenin in nuclear fractions were analyzed by Western blot. D.

Laforin expression (B-D1) in tumor cell line B104-1-1 inhibited the GSK-3β-phosphorylation

and β-catenin nuclear accumulation induced by high dose (500 ng/ml) recombinant Wnt-3A.

E. Increased GSK-3β-phosphorylation and β-catenin nuclear accumulation in the thymocytes

from transgenic mice with lymphoma (Tg-Tu), but not the normal mice (Ntg) and the

transgenic mice yet to develop lymphoma (Tg). Freshly isolated thymi were lysed and

nuclear and cytoplasmic proteins were analyzed for the presence of P-GSK-3β (Ser 9), total

Akt, and nuclear β-catenin. Data shown represent three independent experiments. F. siRNA

silencing of laforin expression in fibroblast cell line EEF8-TQ increases its tumorigenicity.

EEF8-TQ (1×10^6/mouse) infected with lentiviruses containing either vector control or C-

terminal silencing sequence were injected subcutaneously into RAG-2(-/-) mice. The growth

kinetics was recorded over a two-month period. Data shown represent two independent

experiments with 3 mice per group. The insert shows the laforin protein levels of the cell

lines used. Similar results were obtained with independent transfectants from different

experiments (Supplemental Fig. 7). G. Increased tumorigenicity of *EPM2a* silenced EEF8-

TQ cell line is eliminated by expression of dominant negative TCF mutant (ΔTCF). As in F,

except that the laforin-silenced EEF8-TQ cell line super-transfected with either vector alone

(V) or ΔTCF were used. The data shown are tumor growth kinetics with 5 mice per group.

Essentially identical results were obtained in a repeat. The levels of laforin and the ΔTCF

protein were determined by Western blot, and a control cell line expressing both ΔTCF and

laforin was used as control.

Supplemental figure legends

Fig. S1. Over-expression of genes adjacent to TCR transgene integration site does not lead to tumorigenesis. A. Genomic organization of *EPM2a* and the only two other genes within 300 Kb of the integration site on chromosome 10. The cDNA designations are based on Celera database. B. Expression of the two adjacent genes in non-transgenic littermates (Ntg), transgenic mice without tumor (Tg) and transgenic mice that developed tumor (Tg-Tu), as determined by RNase protection assay. C. Summary of observation period of 8 transgenic founder mice and 12 offspring of the founder 6, all express mCG16603 under the control of the proximal *lck* promoter. D. Offspring of founder 6 (mouse F392) overexpresses mCG16603 gene, as determined by real-time PCR. Data shown are means and SD of triplicate samples and has been repeated twice.

Fig.S2. Over-expression of laforin selectively prevents PDGF-induced phosphorylation of GSK-3β. Vector or laforin-V5 transfected NIH3T3 cells were stimulated with PDGF for given periods of time. The activation of Akt (anti-p-Akt, Ser 473) and GSK-3β (anti-p-GSK-3β, Ser 9) were analyzed by Western blot. The amount of protein loaded was revealed using the total Akt as determined by Western blot. Summaries of data from three independent experiments presented as the means +/- S.D. of the relative amounts of phosphorylated proteins at 30 minutes after PDGF-treatment. The films were scanned using CanoScan LiDE 30 (Canon USA Inc, Salt Lake City, UT), and the intensity of the band was determined using SigmaScan Pro 4 for windows (SPSS Inc., Chicago, IL). The signals of phosphorylated Akt or GSK-3β were divided by the signals of total Akt or GSK-3β. These ratios were then

normalized over those from PDGF-treated vector-transfectants (1.0). The statistical

significance was determined by student t-test.

Fig. S3. Dose-dependence and specificity of *EPM2a* siRNA effect. A. Two different knock

down constructs resulted in different degrees of laforin knock-down (upper panel) and

biological effect on GSK-3β phosphorylation at Ser 9 (lower panel). B. Overcoming

inhibition of GSK-3β phosphorylation in laforin-knock down cells by human laforin, which

had two basepair mis-match in the C-terminal silencing sequence. Note that the anti-laforin

antibody was cross-reactive with both mouse and human laforin.

Fig. S4. Laforin-GSK-3β association was unaffected by PDGF stimulation and did not require

phosphastase activity of laforin. Experiments were done as in Fig. 6E, except that cells were

stimulated with PDGF or medium for 30 min. prior to lysis and immunoprecipitation with

anti-GSK-3β antibody.

Fig. S5. Specificity and phosphatase activity of laforin expressed in *E. coli*. Recombinant

GSK-3β or Bad was phosphorylated by constitutively activated Akt in the presence of ATP.

Wild type or mutant laforin proteins (0.5 or 1.0 μg/sample) were added to the mixture after

the phosphorylation was complete. The phosphatase activity was determined by Western blot

using either anti-p-Ser 9 GSK-3β or anti-p-Bad (S112) antibodies. Data shown represent

three independent experiments.

Fig. S6. A. In the presence of a suboptimal dose of PMA, Wnt3A induced GSK-3β

phosphorylation at Ser 9 position. NIH3T3 cells were deprived of serum for 2 hours and then

treated with 10 ng/ml of Wnt3A and given doses of PMA (μM). The significance of PKC

activation was verified by a 30 min pre-treatment with 50 nM of PKC inhibitor GÖ98. B.

Phosphatase activity of larofin was not induced by PMA. The stable *EPM2a-V5* transfected

NIH3T3 clone D14 was treated with PMA (0.5 µM) for 30 min. before lysis for

immunoprecipitation with anti-V5 antibody. Phosphatase activity in the immunoprecipitate

was detected using p-NPP as substrate. The NIH3T3 transfected with vector was used as

control. C. PMA and Wnt did not modulate association between laforin and GSK-3β. Clone

D14 was deprived of serum for 2 hour and was then either left untreated or treated with 0.5

µM of PMA and/or with 20 ng/ml Wnt3A for 1 hour. The cells were lysed,

immunoprecipitated with anti- GSK-3β, and probed with either anti-GSK-3β or anti-V5

antibodies in Western blots.

Fig. S7. RNAi silencing of laforin expression in fibroblast cell line EEF8-TQ increases its

tumorigenicity. EEF8-TQ was infected with lentiviruses containing either vector control (V2,

empty circle) or C-terminal silencing sequence (C5, solid square) as detailed in methods. The

insert shows the laforin protein level of representative clones from each group. The control

and silenced clones of EEF8-TQ cells (1×10^6/mouse) were injected subcutaneously into RAG-

2(-/-) mice. The incidence and growth kinetics were recorded over a two-month period. Data

shown represent two independent experiments. In combination, tumors were detected in all 8

mice that received the silenced clone, but in none of the 8 mice that received the control clone.

Fig. 1

A

B

Integration site

TCR-Cα

Query: 67   tgatccactcccagcatagaggaaaggtgaa   95
            ||||||||||||||||||||||||||||||
Sbjct: 577411 tgatccactcccagcatagaggaaaggtgaa   577439

Chromosome 10

Query: 96   cacaaggtggtgttgagaagaactgag   122
            |||||||||||||||||||||||||||
Sbjct: 3826453 cacaaggtggtgttgagaagaactgag   3826427

GATCCACTCCCAGCATAGGAAAGGTGAACACAAGGTGGTGTTGAGAAGAACTGAG

C

TCR α chain and β chain transgene junction

TCR Cα →   ← TCR Vβ

Integration site

D

TCRα

Integration site

Nsil   Nsil   Nsil

Chro 10
Tg allele

Probe

Chro 10
WT allele   Nsil   Nsil

5.3 Kb

NTg   Tg

5.3Kb —

2.5Kb —

E

Integration site
(8,243,046)

mCG16603

8232K   Epm2a (mCG16610)

16Kb   46Kb   11Kb   115Kb

Fig. 2

Fig. 3

A

Epm2a CpG Island

Exon 1

-443   +68   +782

ATG

278bp(11) 124bp(21)

333bp(45)

222bp(25)

B

Tg-Tu
4012 (8)
4023 (9)
4026 (10)
4217 (10)
4517 (10)
4605 (10)

Tg
11992 (10)
11993 (10)
11996 (10)
12029, 12030 (15)
12032

100% 90% 80% 70% 50% 0%

Fig. 4-1

Fig. 4-2

Fig. 5-1

Fig. 5-2

Fig. 5-3

Fig. 6-1

Fig. 6-2

Fig. 7-1

Fig. 7-2

Fig. 7-3

G

F

Tumor volume (mm³)

Days after injection

Integration site
(8,243,046)

A

mCG140768

8042K   8108K

66Kb   62Kb

mCG16603

8170K   8186K

16Kb   46Kb

8232K

11Kb

EPM2A (mCG16610)

8347K

115Kb

B

NTg   Tg   Tg-Tumor

mCG16603

GAPDH

mCG140768

GAPDH
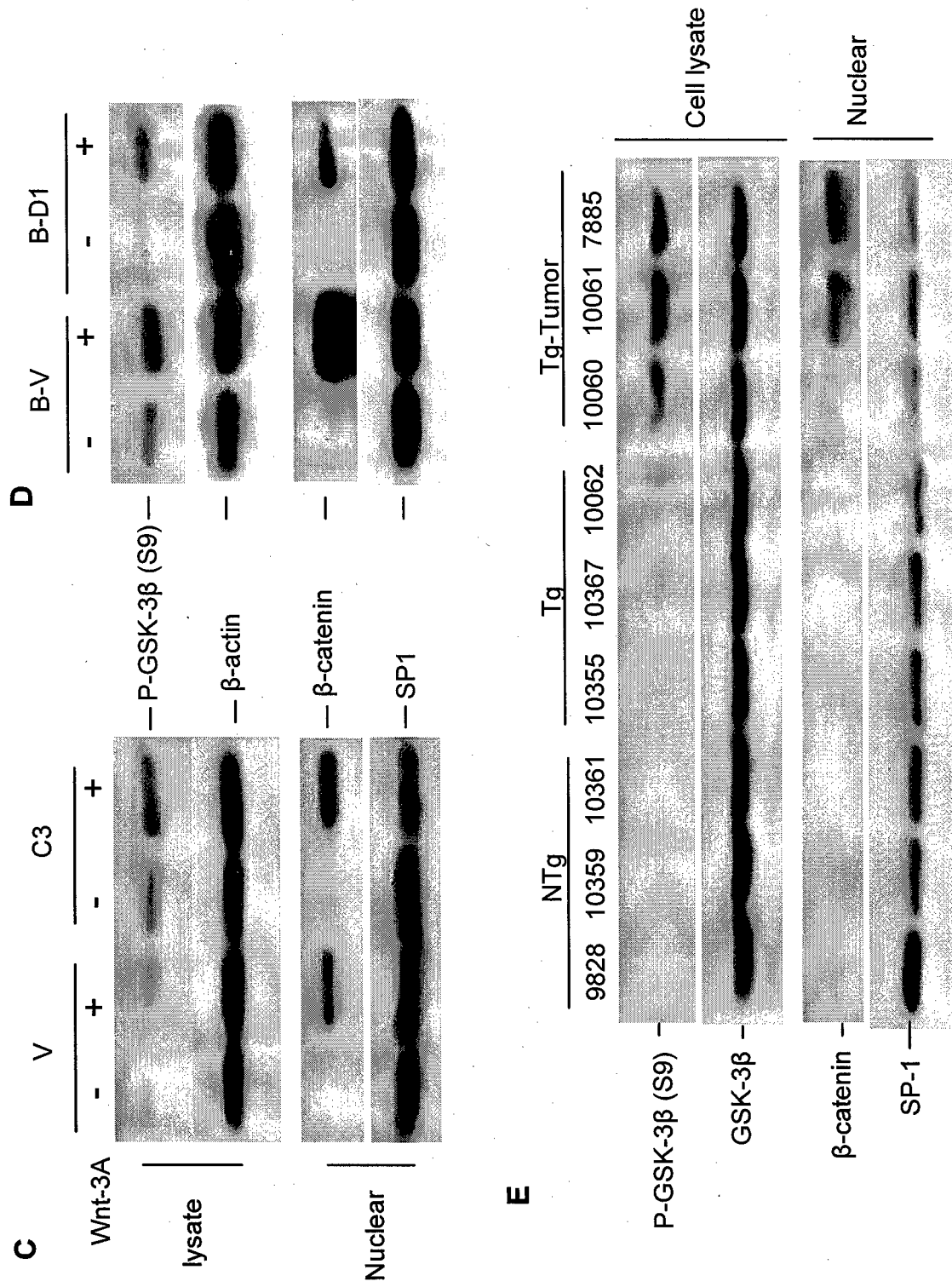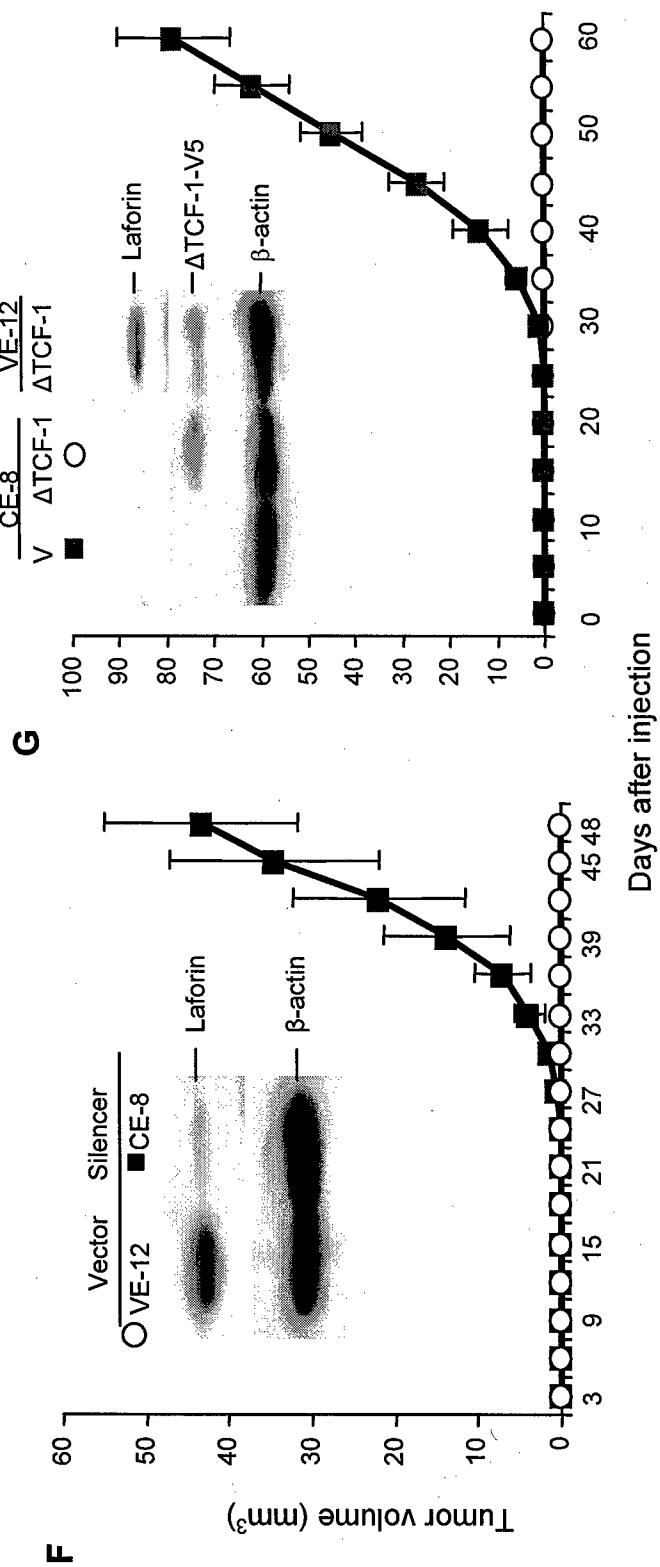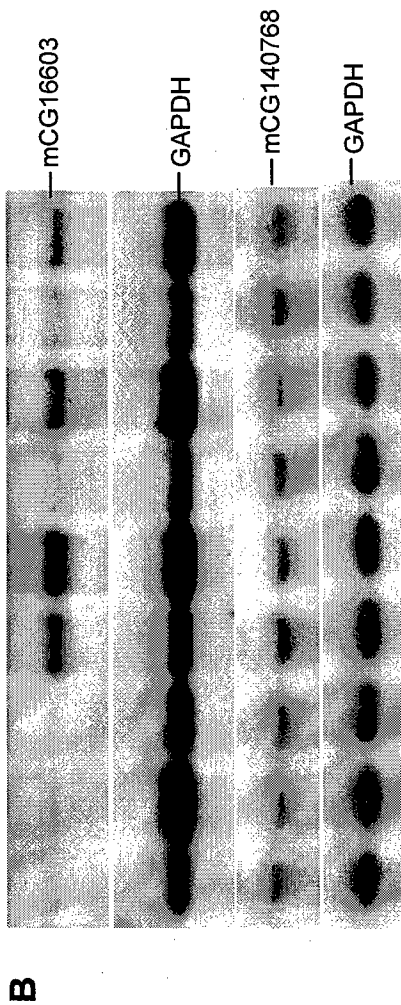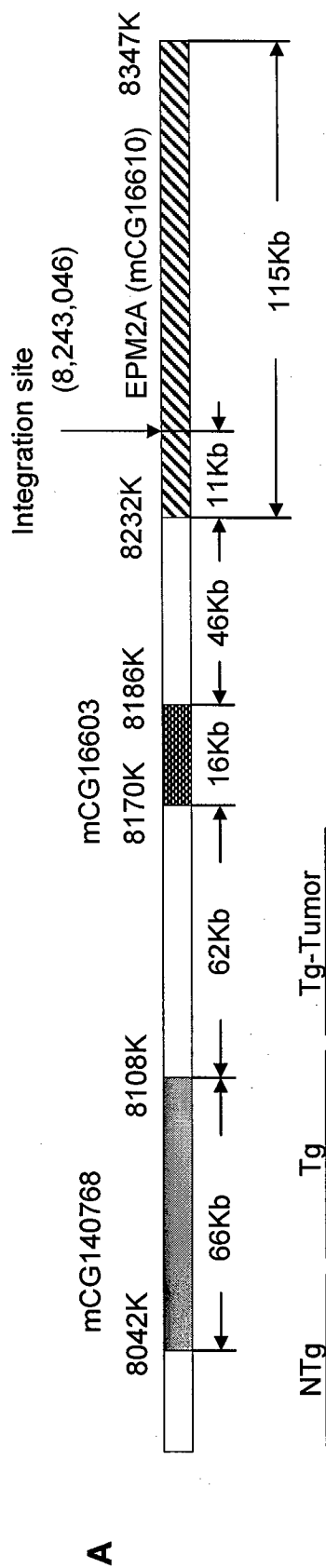
C mCG16603 transgenic mice

Founder No.	Observed Period (wk)	Lymphoma
1	65	No
2	93	No
3	72	No
4	67	No
5	96	No
6	84	No
7	63	No
8	64	No
12 offspring from founder No.6	45-61	No

D

Ratio VS HPRT

0.3 0.25 0.2 0.15 0.1 0.05 0

F384(-)   F392(+)   TGB(-)   TGB(+)
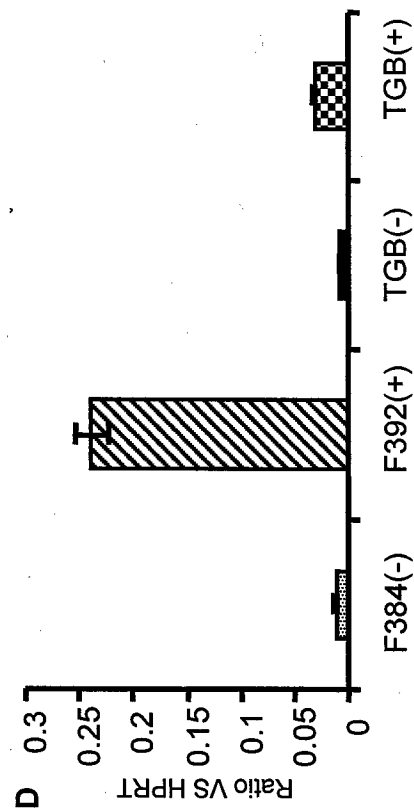
Fig. S1

Fig. S2

Fig. S3

Fig. S4

Fig. S5

Fig. S6

Fig. S7